

# Simulation of seasonal precipitation and raindays over Greece: a statistical downscaling technique based on artificial neural networks (ANNs)

K. Tolika,<sup>a</sup> P. Maheras,<sup>a,\*</sup> M. Vafiadis,<sup>b</sup> H. A. Flocas<sup>c</sup> and A. Arseni-Papadimitriou<sup>a</sup>

<sup>a</sup> Department of Meteorology and Climatology, University of Thessaloniki, Greece

<sup>b</sup> Division of Hydraulics, Faculty of Technology, University of Thessaloniki, Greece

<sup>c</sup> Laboratory of Meteorology, Department of Applied Physics, University of Athens, Greece

## Abstract:

A statistical downscaling technique based on artificial neural network (ANN) was employed for the estimation of local changes on seasonal (winter, spring) precipitation and raindays for selected stations over Greece. Empirical transfer functions were derived between large-scale predictors from the NCEP/NCAR reanalysis and local rainfall parameters. Two sets of predictors were used: (1) the circulation-based 500 hPa and (2) its combination along with surface specific humidity and raw precipitation data (nonconventional predictor). The simulated time series were evaluated against observational data and the downscaling model was found efficient in generating winter and spring precipitation and raindays. The temporal evolution of the estimated variables was well captured, for both seasons. Generally, the use of the nonconventional predictors are attributed to the improvement of the simulated results. Subsequently, the present day and future changes on precipitation conditions were examined using large-scale data from the atmospheric general circulation model HadAM3P to the statistical model. The downscaled climate change signal for both precipitation and raindays, partly for winter and especially for spring, is similar to the signal from the HadAM3P direct output: a decrease of the parameters is predicted over the study area. However, the amplitude of the changes was different. Copyright © 2006 Royal Meteorological Society

KEY WORDS statistical downscaling; artificial neural network; precipitation; raindays; Greece; general circulation model

Received 5 December 2005; Revised 2 June 2006; Accepted 17 September 2006

## INTRODUCTION

Currently general circulation models (GCMs) remain the most appropriate tool to estimate future global scale climate changes for an atmosphere enhanced with greenhouse gases. Despite their unquestionable usefulness, GCMs have been proved to be ineffective in simulating surface variables at the catchment-scale due to their spatial resolution of a few hundred kilometers. This mismatch-scale problem becomes more intense when a study is focused on precipitation, which strongly depends on subgrid-scale processes (Wilby and Wigley, 2000) and on regions with complex and sharp orography (Schmidli *et al.*, 2005). The need for regional rainfall scenarios for impact and hydrological studies leads to a wide development of several downscaling techniques to bridge the gap between the large-scale GCM information and local scales.

These downscaling processes are divided into two general categories: (1) dynamical processes, using physically based regional climate model (RCMs), and (2)

statistical–empirical processes providing empirical transfer functions to define and relate in a statistical way the independent variable (predictors) with the dependent variables (predictants). Many different statistical methods have been employed, such as: canonical correlation analysis (CCA) (von Storch *et al.*, 1993; Gyalistras *et al.*, 1994; González-Rouco *et al.*, 2000; Busuioc *et al.*, 2001), linear and multiple regression (Kidson and Thompson, 1998; Kilsby *et al.*, 1998; Kysely, 2002), nonparametric models (Corte-Real *et al.*, 1995), fuzzy logic neural networks (Cavazos, 1997; Crane and Hewitson, 1998; Trigo and Palutikof, 2001; Marzban, 2003; Knutti *et al.*, 2003; Tatli *et al.*, 2004), and singular value decomposition (Busuioc *et al.*, 1999; von Storch and Zwiers, 2001).

The main advantages of a statistical downscaling approach are the limited computer time and computing resources needed, the fact that they are applicable to output data from different GCMs and that they can be transferred in different regions (Goodess and Palutikof, 1998; Solman and Nunez, 1999; Timbal *et al.*, 2003). Also, in their latest study Goodess *et al.* (2006) noted that an empirical downscaling technique could contribute to the evaluation of the GCM or RCM skill with respect to its ability to reproduce the predictor variables together with its relationships with the predictants.

\* Correspondence to: P. Maheras, Department of Meteorology and Climatology, School of Geology, Aristotle University of Thessaloniki, 54124 Greece. E-mail: maheras@geo.auth.gr

In this study, a statistical downscaling model based on an artificial neural network (ANN) is employed. Our objective is to evaluate its skill in generating seasonal precipitation totals and raindays in Greece to apply it afterwards using the output data from a GCM for the present (control run) and the future (scenarios) period to estimate future climate changes. It is noteworthy that the evaluation of precipitation data is quite complicated owing to the fact that the precipitation regime in Greece presents highly irregular behavior on both the spatial and temporal scale (Maheras and Anagnostopoulou, 2003). It is well accepted that the main physical and physico-geographical factors controlling the spatial distribution of precipitation over Greece are: the atmospheric circulation, mountains in the west and east, the Mediterranean Sea-surface temperature distribution, rehumidification of the air masses crossing the Aegean Sea and land and sea interactions (Xoplaki *et al.*, 2000). Furthermore, the complex orography, the valleys along which the air masses are canalized and the large number of islands result in an even lower predictability of precipitation from the direct output of a coarse-scale GCM and the application of a downscaling technique is considered to be essential for the estimation of the changes of the aforementioned rainfall parameters in future climate conditions.

## DATA AND METHODOLOGY

### Data sets

The data employed in this study include daily precipitation data from 22 stations evenly distributed all over Greece (Figure 1(a, b)) for the period 1958–2000. These data series are complete without missing values. The station data were checked for homogeneity with the aid of the Alexandersson (1986) homogeneity test, on a monthly basis and for each station separately. The results of the test verified that the data of all of the stations are homogeneous.

For the purpose of downscaling, large-scale predictor fields from the national centers for environmental prediction—and national center for atmospheric research (NCEP–NCAR) reanalysis (Kalnay *et al.*, 1996) were employed. More specifically, daily values of 500 hPa, 700 hPa geopotential and 1000–500 hPa thickness daily data were used, covering the European area from 30°N to 55°N and from 0° to 32.5°E with a spatial resolution of 2.5° × 2.5° for the period 1958–2000. Also, daily surface specific humidity and raw precipitation data (NCEP) for a 24-point grid set were considered over Greece (Figure 1(c)), with a spatial resolution of 2.5° × 2.5° for the same time period. The use of the reanalysis data as the large-scale predictors gives the researcher an advantage in verifying the downscaling results against observational data with minimal interference from uncertainties in the simulated large-scale circulation (Salathé, 2003).

The HadAM3P circulation (500 hPa, 700 hPa and thickness (1000–500 hPa), surface specific humidity and

precipitation fields, for the same windows and resolution as the NCEP data, were used as inputs in the ANN model to derive a present day scenario of the seasonal precipitation in Greece. Initially, the spatial resolution of the examined atmospheric model was 1.25° lat × 1.875° long (STARDEX final report (<http://www.cru.uea.ac.uk/projects/stardex>)). Afterwards, the HadAM3P data, used in the study, were regridded to match the NCEP grid with which the statistical downscaling model was trained (resolution 2.5° × 2.5°).

Except for a few changes in physical parameterizations, HadAM3P is similar to the Hadley Center model HadAM3H, which is described in detail by Jones *et al.*, (2001). The resolution of the model is high to provide the atmospheric response to the global sea-surface temperature (SST) and sea-ice changes. It also provides a more accurate simulation of regional climate including Europe, due to a doubling of resolution compared to previous versions of the model. The main improvements are: (a) a more accurate simulation of the strength and position of the north Atlantic storm track and (b) a more realistic representation of clouds and atmospheric humidity with consequent impacts on radiation and precipitation (Pope *et al.*, 2000; Jones *et al.*, 2001). The control run data set is available for the period 1960–1990.

Finally, the HadAM3P scenario data (2070–2100) based on the A2 IPCC SRES scenarios (Cubash *et al.*, 2001), for the aforementioned parameters, are used as predictors to the downscaling model to calculate changes in seasonal precipitation and raindays in Greece being attributed to changes in circulation, specific humidity and raw precipitation in future climate.

Taking into account that summer rainfall in Greece is insignificant and in some cases nonexistent, summer was excluded from the study. Also, although the analysis was carried out for all other three seasons, it was found that the results and the performance of the model was inferior in the case of autumn, in comparison to the other two seasons and especially from winter. Therefore, the downscaling results refer to winter and spring precipitation. Furthermore, this study was extended in analyzing and evaluating our downscaling technique in simulating the seasonal raindays, which were calculated from observed daily precipitation data for a 0.1 mm threshold (Tolika and Maheras, 2005).

At this point it is worth mentioning that a primer evaluation of the success of the HadAM3P in reproducing the general features of one of the main predictors (500 hPa geopotential heights) as well as precipitation and raindays (predictants) in the study area was made by Tolika *et al.*, 2006; Tolika, 2006. As derived from the two studies, the atmospheric model was able to capture and reproduce satisfactorily the relationship between the atmospheric circulation at the 500 hPa level and precipitation, the links between the 500 hPa variability and the precipitation variability, as well as the connections between the precipitation data and circulation types over the Greek area. So, one of the main requirements of all the statistical downscaling methods for the development of scenarios,



prespecified because the ANNs search for the best possible relationship and they derive the best function between the predictors and the predictants (Crane and Hewitson, 1998).

In the context of the STARDEX project (Maheras *et al.*, 2004; Kostopoulou *et al.*, 2005; Goodess *et al.*, 2006), the authors have also applied different downscaling approaches, for example, multi-linear regression, cross-validation or CCA models. So, in the present case, one of the main objectives was the use of a different and more sophisticated approach such as the ANNs for the simulation of precipitation. Moreover, it was considered that a stochastic approach (e.g. autoregressive moving average) could provide satisfactory results for the development of rainfall scenarios (Koutsoukis *et al.*, 2006). However, this kind of technique is not recommended for downscaling purposes and it can provide predictions for only a short period, without the use of GCM data. Since the main scope of the study was the analysis of a statistical downscaling model for precipitation scenarios and for a much longer period (2070–2100), the ANN model was preferred.

The ANN Model used in this study is based on the 'quickprop' algorithm created by Scott Fahlman using Common Lisp and then translated into C by Terry Regier (University of California, Berkley). This algorithm is described in detail by Fahlman (1988). The model adopts a feed-forward configuration and its learning process is based on the back-propagation method (Wasserman, 1989). After having constructed many configurations for this neural network, it was concluded, on a trial and error basis, that the best results were obtained with only one hidden layer, and the optimal number of its nodes was found to be 12 (Figure 2). More specifically, the identification of the best nodes number was done using

different time periods, attempting various sensitivity tests examining both the correlations and the mean values of the simulated time series. It was found that when the whole time period was used both for training and validation, the model provided 'factitious' results. The mean simulated values were almost identical to the observed mean values, but the correlations between the observed and the simulated time series were very low and in some cases even negative.

The 500 hPa geopotential heights were chosen primarily as the independent variable (predictor). Experimentation showed that the ideal spatial window, which would describe the atmospheric circulation that affects precipitation conditions in the study area but would not add noise to the data set, is 0°–32.5°E and 30–55°N. The ANN model is then applied to the years 1958–1978+ 1994–2000 considered as one period (calibration period) while the intermediate years 1979–1993 were used for the validation of the model results (validation period). This choice was made for compatibility with the perfect boundary conditions (Goodess *et al.*, 2006). It should also be noted that the aforementioned periods (calibration–validation) were selected in the context of the STARDEX project and were employed in all the publications derived from that project (<http://www.cru.uea.ac.uk/projects/stardex>, Goodess *et al.*, 2006; Haylock *et al.*, 2006). Although the use of 15 years as a validation period is quite short, given the available time series it was not possible to use a longer validation period.

Before the training process begins, the weights ( $w$ ) were initialized to a small number using a random seed generator. The NET signal (1):

$$NET = \sum x_n w_n \quad (1)$$

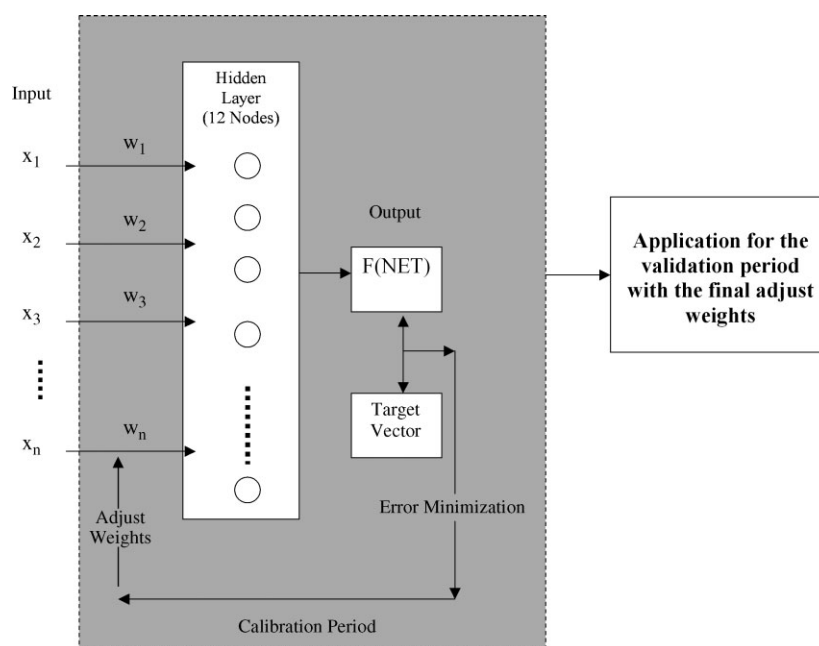


Figure 2. The artificial neural network model used in the study.

is processed by the transfer (activation) function (2)

$$F(NET) = \frac{1}{1 + \exp(-NET)} \quad (2)$$

to produce the output signal. This transfer function is a 'sigmoid function' with values ranging between 0 and 1. Therefore, the target vector of the predictants is 'normalized' taking values between these limits to be compared with the F(NET) signal. The error between the predicted output (F(NET)) and the target vector is estimated using the RMSE (root mean square error, (3)):

$$RMSE = \sqrt{\frac{\sum (F(NET) - t \text{ arg } etvector)^2}{N}} \quad (3)$$

This calculated error is then back propagated and the weights are determined again to minimize the error in the next 'training year'. This procedure ends when the error reaches a minimum value.

#### Performance criteria

Four performance criteria were selected to evaluate the skill of the downscaling model to reproduce seasonal precipitation and raindays: the Spearman-rank correlation coefficient (of the simulated and the observed data), the RMSE between the observed and the simulated data and the mean and standard deviation differences between the two series (Goodess *et al.*, 2006; Kostopoulou *et al.*, 2005). These criteria were calculated on a seasonal basis for each station during the validation period 1979–1993.

#### Selection of the predictors

An attempt was made to find other appropriate predictors, which aimed at the improvement of the simulated precipitation and raindays results of the downscaling model. Wilby and Wigley (2000) presented a comparative study on the predictors used for downscaling of precipitation – there is no rule for that selection as it depends on the decision of each researcher. The circulation-based predictors are the most commonly used, such as geopotential fields at different levels (500 hPa, 700 hPa), 1000–500 hPa thickness field, the sea level pressure (SLP) and specific humidity near the surface (SH) (Cavazos, 1997; Crane and Hewitson, 1998; Busuioc *et al.*, 1999; González-Rouco *et al.*, 2000; Trigo and Palutikof, 2001; Tatli *et al.*, 2004).

Other researchers (Widmann and Bretherton, 2000; Widmann *et al.*, 2003; Salathé, 2003; Schmidli *et al.*, 2005) support that large-scale precipitation, as derived from reanalysis data or from a GCM, could serve as one of the main predictors in the statistical precipitation downscaling. Moreover, Schmidli *et al.* (2005) demonstrated that GCM precipitation integrates all relevant large-scale predictors. Besides, downscaling methods based on GCM precipitation are likely to be less sensitive to stationarity issues than conventional downscaling methods based on circulation-type predictors Schmidli *et al.* (2005).

Table I shows the predictors or sets of predictors that were tested in this study. As mentioned in the previous paragraph, we used the 500 hPa geopotential heights as the only predictor and then its combination with other circulation-type predictors (700 hPa, 1000–500 hPa thickness field). Afterwards, the principal components analysis (PCA) was applied to the geopotential heights as pre-processing of data to reduce the dimensionality and to compress the complicated variability of the original data (Cavazos, 1997). The scores as derived from the application of the S-mode PCA unrotated were used in the statistical model. Also, surface specific humidity was added as a predictor but only for selected grid points nearest to each station used in the study. Finally, raw precipitation data, again for selected grid points, were used as a predictor combined with the 500 hPa scores and the specific humidity values. It should be noted here that for the raindays simulation, the raindays as derived from the NCEP data set were used as a predictor.

Those seven different sets of predictors were applied in the downscaling model and the results were evaluated using the performance criteria hierarchically ordered: high correlation coefficients, low RMSE values, small mean and standard deviation differences. The validation period is 1979–1993.

The simulated results were analyzed separately for each station but owing to limitation of space only the station averaged values of the four evaluation criteria are presented for the reproduction of winter precipitation and winter raindays (Figures 3 and 4). Analogous results were also found for spring. For mean and standard deviation differences, their absolute values were averaged so that positive and negative differences would not be added together and give a false impression of the mean differences.

As can be seen from Figure 3(a), Pred7 presents the highest averaged correlation coefficient with a magnitude that exceeds the value 0.7. The second highest correlation coefficient value is observed using Pred1 while the other predictors presented lower correlations. Concerning RMSE (Figure 3(b)), again Pred7 was found to be as the most suitable predictor, with the lowest RMSE values, followed by Pred1. The combination

Table I. The primary sets of predictors evaluated in the study.

	Predictors	Abbreviations
1	500 hPa	P <sub>500</sub>
2	500 hPa + 700 hPa	P <sub>500_700</sub>
3	500 hPa + (1000–500 hPa) thickness	P <sub>500_thick</sub>
4	500 hPa scores + (1000–500 hPa) thickness scores	P <sub>500sc_thicksc</sub>
5	500 hPa scores + SH grid	P <sub>500sc_SH</sub>
6	500 hPa scores + 700 hPa scores + SH grid	P <sub>500sc_700sc_SH</sub>
7	500 hPa scores + SH grid + Prec/raindays grid	P <sub>500sc_SH_prec/rd</sub>

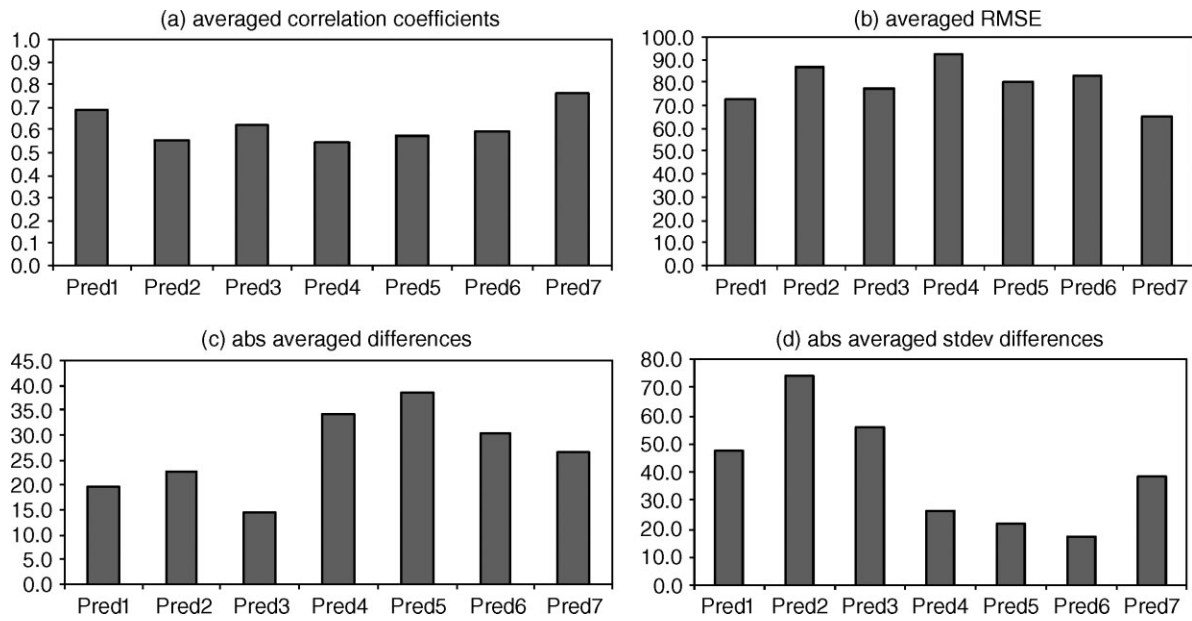


Figure 3. The four performance criteria values for the seven primary sets of predictors, for precipitation in the case of winter. Pred1 = P<sub>500</sub>, Pred2 = P<sub>500\_700</sub>, Pred3 = P<sub>500\_thick</sub>, Pred4 = P<sub>500sc\_thicksc</sub>, Pred5 = P<sub>500sc\_SH</sub>, Pred6 = P<sub>500sc\_700sc\_SH</sub>, Pred7 = P<sub>500sc\_SH\_prec</sub>.

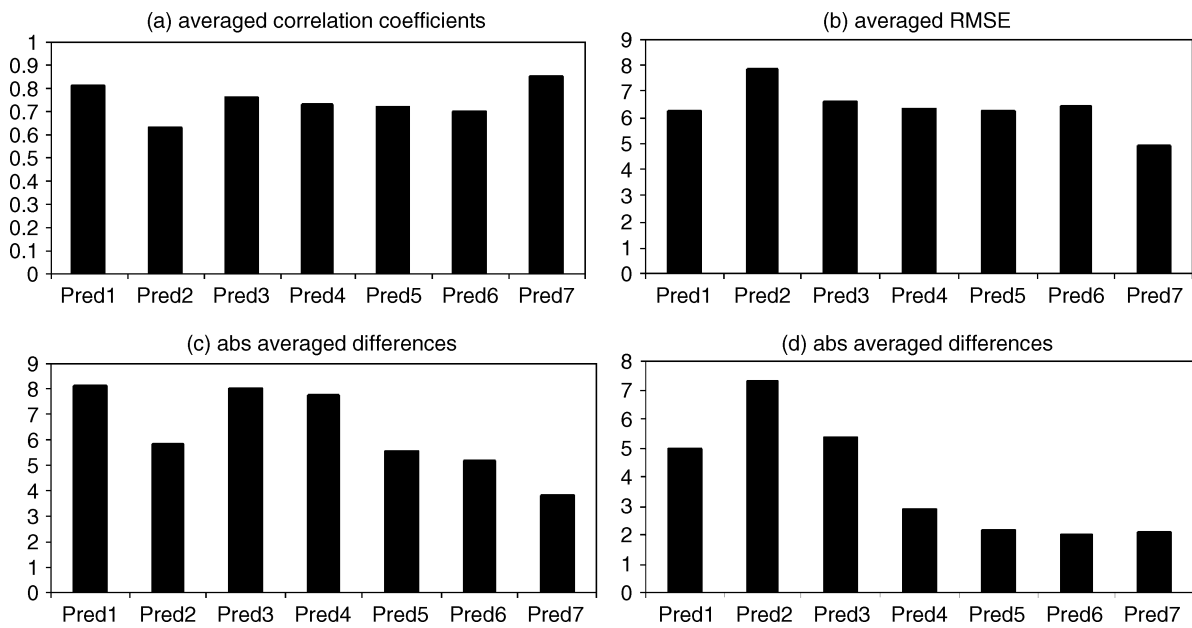


Figure 4. As in Figure 3 but for winter raindays.

of the geopotential field 500 hPa and the thickness field (1000–500 hPa) (Pred3) gave the smallest averaged differences and the simulation of the variability of winter precipitation was better when 500 hPa and 700 hPa scores with specific humidity (Pred6) were used as predictors in the downscaling model (Figure 3(c,d)).

In the case of the raindays reproduction (Figure 4(a–d)) it is obvious that Pred7 is the superior predictor since the simulated results returned the strongest correlations with the observed data, the lowest RMSE values and the smallest mean differences. Also the simulation of the variability of the raindays time series was satisfying.

Therefore, it was found that the combination of 500 hPa scores with selected SH and raw precipitation/raindays grids is the most efficient predictor in generating local scale precipitation and raindays series in the Greek area. Also, it must be noted that the performance of the ANN model using as a single predictor the 500 hPa was quite satisfactory as Pred1 presented high correlation coefficients and low RMSE values. Thus, it was decided that these two predictors, one circulation based (Pred1) and the other a combination of three parameters (Pred7) would be applied and analyzed analytically in this study. Hereafter, the two sets of predictors will be used with their abbreviations Predictor 1 = P<sub>500</sub> and Predictor 2 = P<sub>500sc\_SH\_prec/rd</sub>.

## RESULTS

*Precipitation (validation period 1979–1993)*

Figure 5 displays the correlation coefficients between the observed and the simulated data, for each station, during the validation period 1979–1993 for the two seasons. During winter (Figure 5(a)), it becomes clear that the correlation coefficients for both predictors are high. Regarding  $P_{500}$ , the correlation coefficients vary between 0.3 (Athens) and 0.9 (Agrinio, Ioannina, Kerkyra, Tripoli). Using Predictor 2 ( $P_{500sc\_SH\_prec}$ ), the results improved since higher correlation coefficients were found in 12 stations. In five stations the values of the correlation coefficients remained the same, while in the rest of the stations (five) they were smaller. Their values vary from 0.4 (Kozani) to 0.9 (Agrinio, Chania, Kalamata, Milos, Skyros and Tripoli).

In spring, the correlations were smaller than in winter but again the results using  $P_{500sc\_SH\_prec}$  were more satisfying: the values of the correlation coefficients increased in 11 stations and they vary between 0.2 (Skyros) and 0.7 (8 stations). It should be mentioned that the employment of  $P_{500}$  resulted in correlation coefficients of 0.8 for two stations (Agrinio and Mytilini) (Figure 5(b)).

Another way of assessing our model ability in reproducing the seasonal precipitation was to examine the temporal variability by averaging spatially the simulated and observed results and by calculating the correlation coefficients between the time series. According to Figure 6(a) where the time series are displayed for winter,

the employment of both predictors reproduced very satisfactorily the precipitation during the period 1979–1993. The correlation coefficients between the simulated and the observed data reach the values of 0.89 and 0.96, respectively. In spring, the downscaled results yield also quite high correlation coefficients (0.74 for obs- $P_{500}$ , 0.80 for obs- $P_{500sc\_SH\_prec}$ ), but the simulated precipitation is generally underestimated, especially when the  $P_{500}$  is used (Figure 6(b)).

Furthermore, Table II shows the differences, and the percentage of differences (%), between the simulated and the observed data for all stations. Negative differences can be detected in winter for  $P_{500}$ , except for the stations of Ioannina, Mytilini and Skyros, where precipitation is overestimated (positive differences). None of these differences were found to be statistically significant. It is worth noting that when winter precipitation was simulated using  $P_{500sc\_SH\_prec}$ , the reconstructed results were overestimated for nine stations (positive differences) while for the rest of the stations the differences remained negative. The results were statistically significant for two stations, presenting positive differences (Skyros (48%) and Thessaloniki (49.4%)) and for the station of Kythira (–13.8%) with negative differences.

During spring, the downscaling procedure using  $P_{500}$  underestimates precipitation in all the stations. These negative differences are statistically significant for nine of them. For the stations of Attica (Athens and Elliniko), this underestimation reaches –39% (Table II). The  $P_{500sc\_SH\_prec}$  precipitation appears overestimated for ten

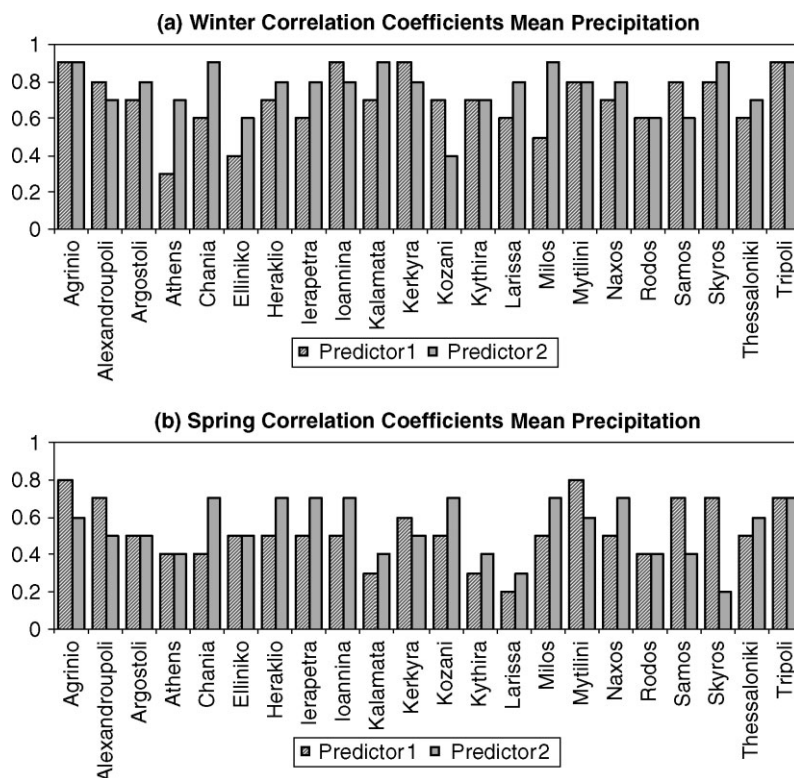


Figure 5. Correlation coefficient values (sim-obs) for the two selected predictors, for winter and spring precipitation. Validation period 1979–1993. Predictor 1 =  $P_{500}$  (striped bars), Predictor 2 =  $P_{500sc\_SH\_prec}$  (gray bars).

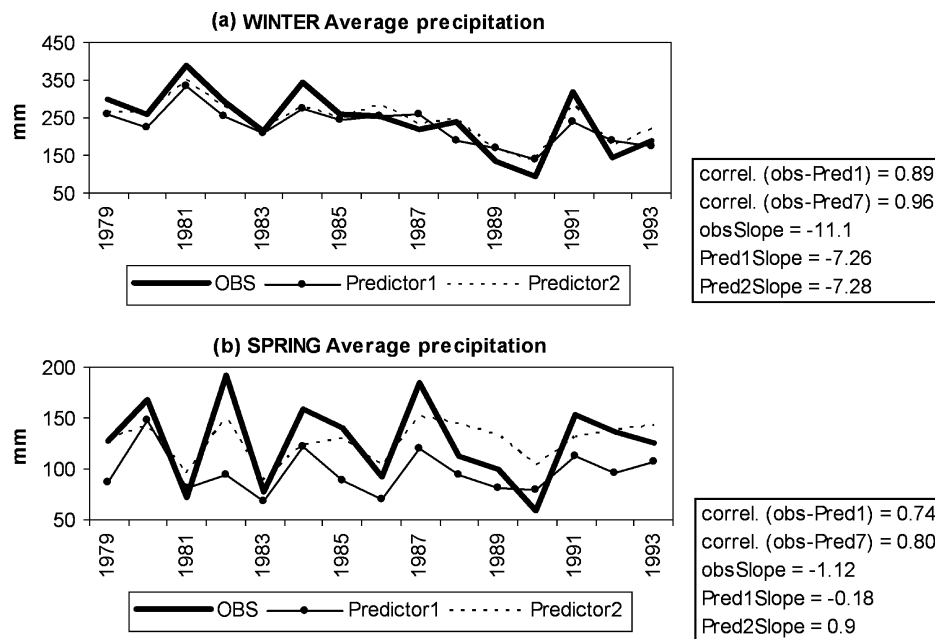


Figure 6. Observed (OBS) and simulated (Predictor 1, Predictor 2) spatially averaged precipitation over the 22 stations in the study in the case of winter (a) and spring (b) for the validation period 1979–1993. The correlation coefficient values between the simulated and the observed data as well as the slope values of each series are given in the box for each case.

Table II. Seasonal precipitation differences and percentage of differences (in italics) between the simulated and the observed data (Sim-Obs) for each station for the two predictors for the validation period 1979–1993. The differences (shaded) are statistically significant ones (Student's *t*-test).

	Winter				Spring			
	P <sub>500</sub>		P <sub>500sc_SH_prec</sub>		P <sub>500</sub>		P <sub>500sc_SH_prec</sub>	
	Sim-Obs	%	Sim-Obs	%	Sim-Obs	%	Sim-sObs	%
Agrinio	-14.8	-4.6	-10.9	-3.4	-39.6	-22.3	-20.3	-11.4
Alexandroupoli	-3.0	-1.8	-12.7	-7.7	-9.5	-9.0	73.7	70.0
Argostoli	-22.7	-6.8	32.0	9.5	-21.3	-14.1	-28.0	-18.6
Athens	-19.1	-14.3	-9.7	-7.2	-41.4	-39.0	-32.8	-30.9
Chania	-26.6	-8.9	44.7	14.9	-25.6	-22.4	-45.9	-40.1
Elliniko	-22.1	-16.3	-18.0	-13.3	-39.6	-38.5	-33.4	-32.5
Heraklio	-11.6	-5.2	-21.0	-9.4	-21.9	-22.9	-33.6	-35.2
Ierapetra	-42.5	-17.4	-25.8	-10.6	-10.6	-14.6	-22.1	-30.5
Ioannina	22.9	6.7	21.6	6.3	-58.7	-24.7	16.6	7.0
Kalamata	-5.2	-1.6	-32.9	-10.3	-45.7	-30.1	57.1	37.6
Kerkyra	-0.4	-0.1	32.4	9.1	-28.7	-15.4	28.4	15.3
Kozani	-4.8	-4.8	1.2	1.2	-20.3	-15.2	-5.2	-3.9
Kythira	-35.3	-13.1	-37.3	-13.8	-34.9	-34.7	2.4	2.4
Larissa	-19.3	-18.0	26.8	25.0	-34.0	-28.2	56.0	46.5
Milos	-12.4	-5.9	1.9	0.9	-27.7	-31.6	-12.4	-14.1
Mytilini	23.2	7.9	-4.1	-1.4	-22.8	-17.0	51.1	38.2
Naxos	-53.5	-26.9	-2.0	-1.0	-17.6	-24.4	-2.1	-2.9
Rodos	-26.8	-7.5	-37.5	-10.4	-33.1	-28.4	-34.0	-29.2
Samos	-32.9	-8.3	-57.9	-14.7	-35.6	-24.2	-42.9	-29.1
Skyros	0.6	0.4	74.81	48.0	-18.1	-22.1	10.7	13.1
Thessaloniki	-9.7	-9.5	50.2	49.4	-26.9	-21.7	14.6	11.8
Tripoli	-26.9	-8.9	-32.3	-10.7	-51.0	-28.6	8.2	4.6

stations mainly in western and northern Greece. In the rest of the stations, rainfall is underestimated. The results were found to be statistically significant in eight stations.

Concerning variability simulation, the differences of the standard deviation values showed that the model employing both predictors did not to generate manage the standard deviation of precipitation sufficiently during the selected seasons (not shown). The differences are negative, suggesting that the variability of the simulated data is significantly lower. However, it should be mentioned that  $P_{500sc\_SH\_prec}$  presented better results (smaller st dev differences) than  $P_{500}$ , in most of the stations. This could also be reinforced by the fact that when the  $F$ -test (variance control at a level of significance  $\alpha = 0.01$ ) was applied, the percentage of the stations with statistically significant differences was much higher in the case of  $P_{500}$ .

Another measure of skill of the downscaling model to reproduce the seasonal precipitation is the RMSE. It is mentioned that the smaller the RMSE values, the better the performance of the model. From the graphs in Figure 7, it can be seen that the nonconventional method ( $P_{500sc\_SH\_prec}$ ) improves the results in many stations since smaller RMSE values were found. During both winter and spring, 15 out of the 22 stations presented lower RMSE than in the case of  $P_{500}$ .

#### *Raindays (validation period 1979–1993)*

The reproduction of the seasonal raindays for the validation period was superior to the simulation of the mean seasonal precipitation. Figure 8 depicts the correlation coefficients between the simulated and the observed raindays for all stations during the two seasons. Both methods ( $P_{500}$  and  $P_{500sc\_SH\_rd}$ ) were very effective in generating rainfall days during winter. The correlation coefficient values exceed the magnitude of 0.8 in most of the stations (Figure 8(a)). In spring, the results are also quite satisfying; however, with lower correlation coefficient values as compared to winter. In the case of  $P_{500}$ , these values range from 0.4 to 0.8. Applying  $P_{500sc\_SH\_rd}$  in the downscaling model, nine stations presented higher values, another nine presented the same correlation values and in only four stations were the results worse (Figure 8(b)).

Concerning the temporal variability of the simulated raindays during the validation period, it becomes obvious that in the case of winter both  $P_{500}$  and  $P_{500sc\_SH\_rd}$  generate well the raindays time series (Figure 9(a)). The correlation coefficients between the simulated and observed series exceed the value of 0.9. Especially for  $P_{500sc\_SH\_rd}$ , the two series are almost identical after 1986, while the  $P_{500}$  raindays are underestimated. In spring, both methods perform satisfactorily with correlation coefficients 0.83 (for  $P_{500}$ ) and 0.92 (for  $P_{500sc\_SH\_rd}$ ). The  $P_{500}$  method underestimates the spring raindays but the variability of the simulated series resembles that of the observed data. The  $P_{500sc\_SH\_rd}$  method simulates better raindays (Figure 9(b)). Also, the slope values demonstrate that the simulated series trend is in the

same direction to the observed trend and their magnitudes are close to the observed ones, especially during spring.

From Table III, which presents the differences and the percentage (%) of these differences between the simulated and observed raindays of each station during the validation period, it becomes evident that the model with  $P_{500}$  underestimates the observed values (negative differences, an average underestimation  $-25\%$ ) while the results are statistically significant in most of the stations. In the case of  $P_{500sc\_SH\_rd}$ , the reconstructed raindays are also underestimated in 14 stations while in the rest of them a smaller overestimation is observed. In spring, an underestimation of the  $P_{500}$  simulated values becomes evident with statistical significance in 12 of the stations in the study. The results using  $P_{500sc\_SH\_rd}$  were found improved (smaller differences) and only the station of Ierapetra presented statistically significant differences (a  $-31.7\%$  underestimation).

Moreover, it can be noted that both downscaling methods generated lower variability than the observed one. In both seasons, it is obvious that the  $P_{500sc\_SH\_rd}$  method manages to approach better the seasonal variability – the calculated differences are smaller than in the case of  $P_{500}$  in almost all stations.

The superiority of  $P_{500sc\_SH\_rd}$  in generating the raindays in the Greek area could be reinforced by the comparison of the RMSE values that have been computed for both methods: for winter all of the stations in the study presented lower RMSE values (better performance) than the ones using  $P_{500}$ . In spring, for more than half of the stations (14 stations) the results have been improved by applying the  $P_{500sc\_SH\_rd}$  to the downscaling model (Figure 10(a–b)).

#### *HadAM3P results for present day scenario 1960–1990-precipitation*

In this section, an attempt is made to generate a present day scenario using data from the atmospheric GCM HadAM3P. The downscaling model was trained for the period 1958–2000 with the aid of NCEP data and afterwards it was applied using the GCM data for the period 1960–1990 for both methods ( $P_{500}$  and  $P_{500sc\_SH\_prec}$ ). The ability and the skill of the HadAM3P in reproducing the links between the chosen predictors and precipitation over the Greek region was assessed by comparing the downscaled results to the observational ones for the period 1960–1990.

The six composed maps on the first two columns of Figure 11 depicts the differences between the predicted and observed seasonal precipitation of the period 1960–1990 using both sets of predictors. Also Table IV presents the percentage of the magnitude of these differences. The application of  $P_{500}$  in the ANN model demonstrates that HadAM3P underestimates winter precipitation in the whole study region. The greatest negative differences are observed in western Greece and the eastern Aegean Sea, areas that are characterized by highest winter precipitation totals. These differences in

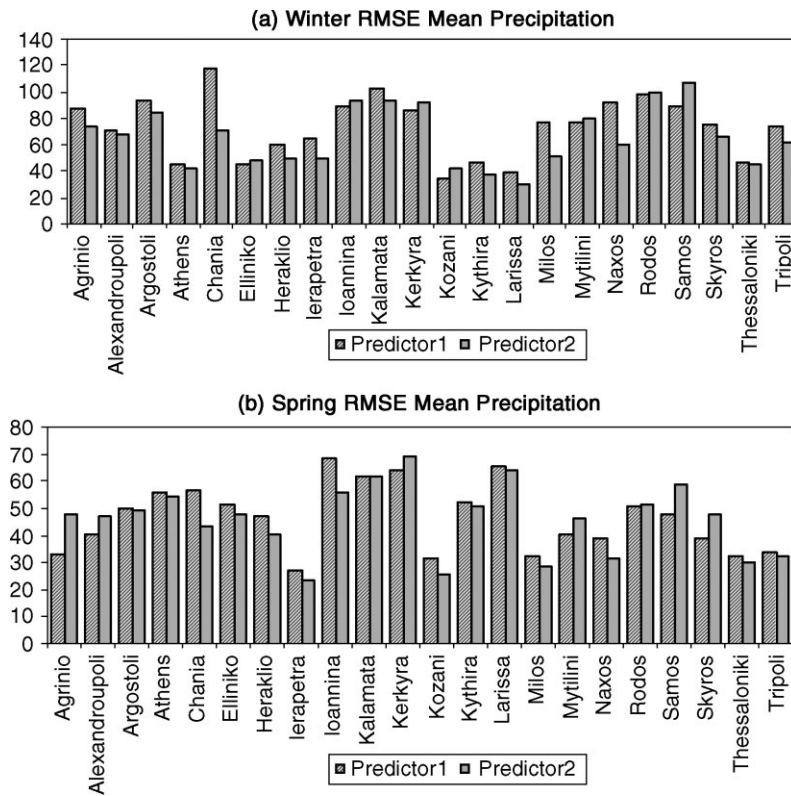


Figure 7. As in Figure 5 but for the seasonal precipitation RMSE values.

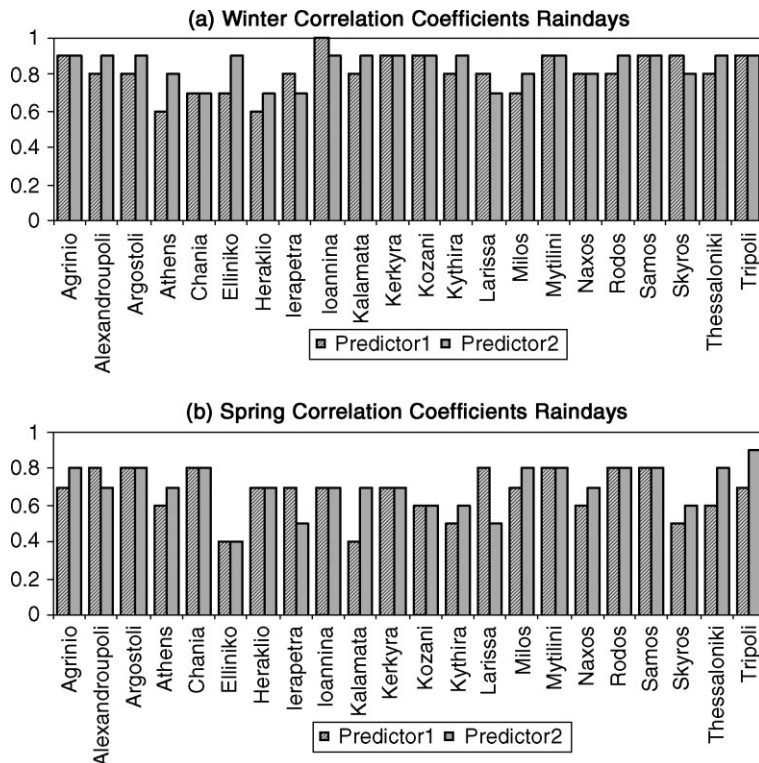


Figure 8. Correlation coefficient values (sim-obs) for the two selected predictors, for winter and spring raindays. Validation period 1979–1993. Predictor 1 =  $P_{500}$  (striped bars), Predictor 2 =  $P_{500sc\_SH\_rd}$  (gray bars).

the aforementioned areas as well as in central continental Greece and in the northern Aegean Sea are statistically significant (Figure 11 (a1)). According to Table IV,

the calculated differences vary from  $-1.4\%$  (Milos) to  $-27.1\%$  (Skyros). The underestimation of winter precipitation could be attributed to the fact that HadAM3P

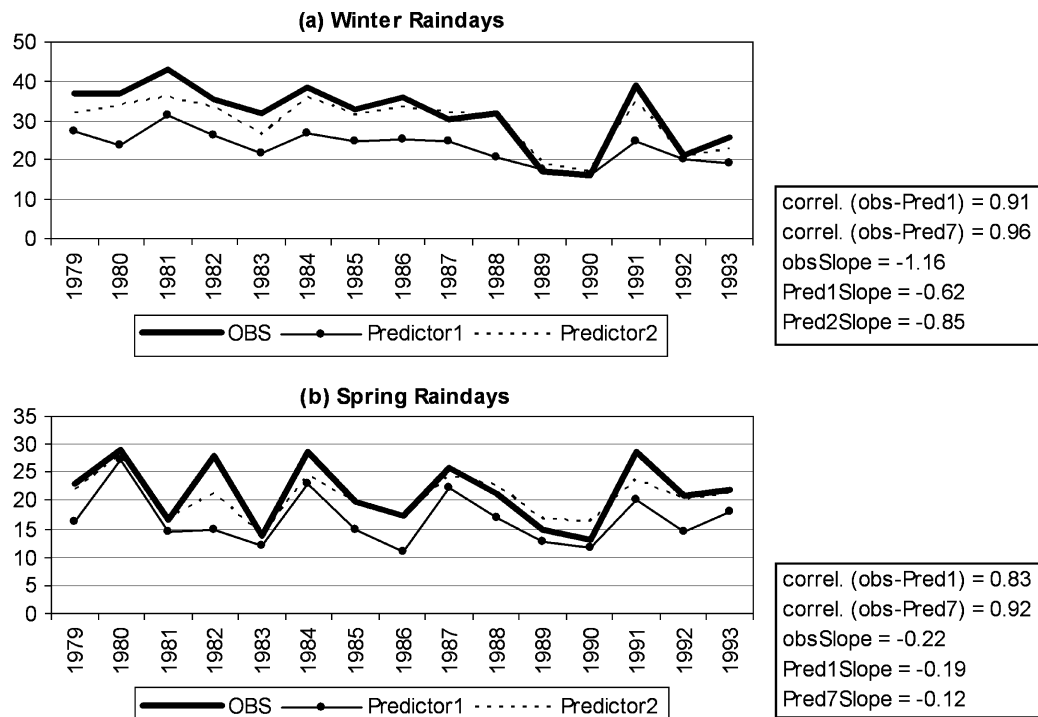


Figure 9. As in Figure 6 but for seasonal raindays.

Table III. As in Table II but in the case of seasonal raindays.

	Winter				Spring			
	P <sub>500</sub>		P <sub>500sc_SH_rld</sub>		P <sub>500</sub>		P <sub>500sc_SH_rld</sub>	
	Sim-Obs	%	Sim-Obs	%	Sim-Obs	%	Sim-Obs	%
Agrinio	-9.3	-26.8	-9.1	-26.3	-7.4	-25.9	1.3	4.6
Alexandroupoli	-2.7	-12.4	-5.4	-24.8	-3.7	-17.8	1.3	6.3
Argostoli	-8.2	-22.0	-8.9	-23.8	-4.5	-19.6	-2.9	-12.6
Athens	-6.7	-26.7	1.0	4.0	-6.3	-30.7	-0.9	-4.4
Chania	-12.7	-31.0	0.3	0.7	-3.9	-21.5	-2.0	-11.0
Elliniko	-6.6	-27.7	-2.2	-9.2	-5.9	-31.4	1.0	5.3
Heraklio	-11.0	-29.8	1.7	4.6	-5.5	-30.8	-2.4	-13.4
Ierapetra	-11.2	-33.0	3.8	11.2	-5.5	-42.5	-4.1	-31.7
Ioannina	-6.9	-20.3	-5.3	-15.6	-5.8	-16.9	-1.6	-4.7
Kalamata	-7.2	-19.4	-4.8	-12.9	-3.4	-14.2	0.0	0.0
Kerkyra	-8.1	-22.1	-4.6	-12.6	-4.4	-16.4	0.6	2.2
Kozani	-8.5	-34.9	5.7	23.4	-5.0	-17.7	-3.9	-13.8
Kythira	-9.7	-27.4	-8.8	-24.9	-5.1	-29.8	3.5	20.4
Larissa	-9.0	-34.6	-1.5	-5.8	-5.8	-21.6	0.1	0.4
Milos	-7.4	-25.1	-1.1	-3.7	-2.7	-21.2	-1.0	-7.9
Mytilini	-6.1	-20.6	-2.7	-9.1	-3.3	-17.2	-3.6	-18.8
Naxos	-8.6	-27.7	-3.2	-10.3	-4.7	-30.4	-4.0	-25.9
Rodos	-8.0	-22.6	1.9	5.4	-4.6	-27.4	-1.0	-6.0
Samos	-8.4	-24.6	-4.3	-12.6	-5.1	-27.7	-3.0	-16.3
Skyros	-3.3	-13.3	3.2	12.9	-3.2	-21.9	0.8	5.5
Thessaloniki	-5.7	-24.2	-5.2	-22.1	-3.3	-12.3	0.2	0.7
Tripoli	-12.3	-33.2	0.9	2.4	-7.3	-23.5	-0.8	-2.6

presents higher geopotential values at 500 hPa than the corresponding NCEP data in the Greek area (not shown). On the other hand, the use of HadAM3P SH

and precipitation ( $P_{500sc\_SH\_prec}$ ) gave different results. The negative differences (underestimation) are limited in Peloponnisos and Crete, while a small overestimation is

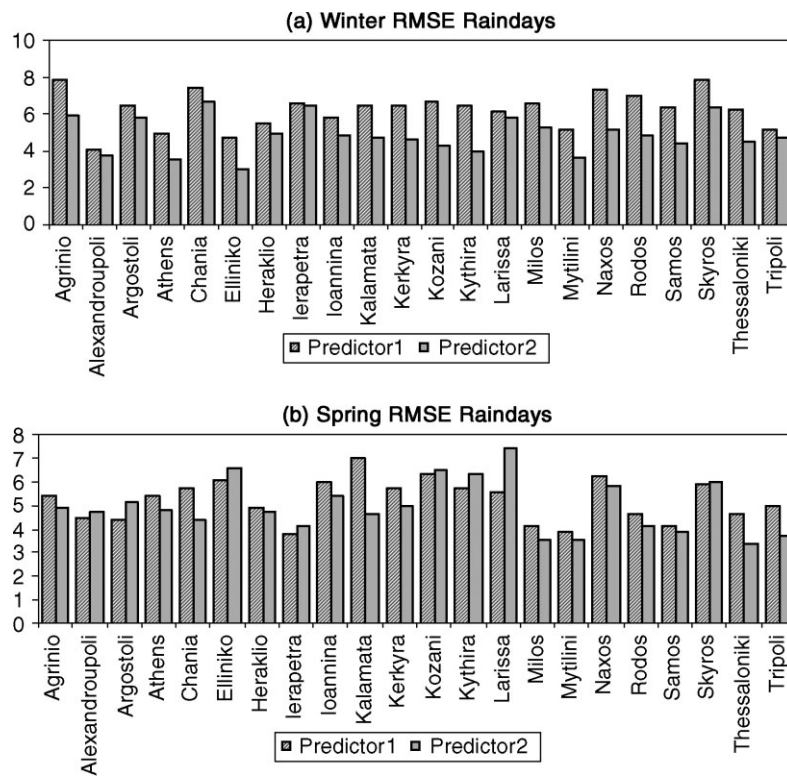


Figure 10. As in Figure 8 but for the seasonal raindays RMSE values.

noted in the rest of the country. The differences are statistically significant only for two stations, Larissa and Tripoli (Figure 11 (a2)).

During spring, the simulated precipitation using HadAM3P  $P_{500}$  is slightly overestimated (small positive differences) in the largest part of Greece. No statistically significant differences were found (Figure 11 (b1)). This overestimation may result from the fact that the values of 500 hPa geopotential height of the GCM are slightly lower than the NCEP ones in the study area. The application of the downscaling model with  $P_{500sc\_SH\_prec}$  showed that the HadAM3P generally overestimates the observed precipitation during the period 1960–1990 (Figure 11 (b2)). The largest positive differences were detected in northeastern Greece with statistically significant differences for the station of Alexandroupoli (18% overestimation, Table IV). In the stations of northwestern Greece, the Ionian Sea and in three island stations (Kythira, Samos, Skyros) of the Aegean Sea, spring precipitation is underestimated (nonstatistically significant negative differences).

The analysis of the differences in the variability (standard deviation) of the simulated and observed precipitation (st dev diff) revealed that the GCM could not capture satisfactorily the variability of the observed time series. The differences between the simulated and the observed st dev values are negative for both the two seasons and for both predictors ( $P_{500}$  and  $P_{500sc\_SH\_prec}$ ) (Figure 11 c1, c2 – d1, c2). This could be attributed partly to the fact that the downscaling model could not generate successfully the

precipitation variability as it was concluded in the previous section.

#### *HadAM3P results for present day scenario 1960–1990 raindays*

The comparison of the downscaled raindays using the HadAM3P data with the observed ones for the period 1960–1990 is presented in Figure 12, while the percentage (%) of the over or underestimation is shown in Table V. Using  $P_{500}$ , it seems that the model underestimates the winter raindays in the whole study region. Western Greece presents the greatest negative differences (–17.2% in the station of Argostoli) and they are statistically significant mainly in the north, west and southwest (Figure 12 (a1)).  $P_{500sc\_SH\_rd}$  gave quite different results: The raindays are overestimated in the larger part of the Greek area and especially in the south where the differences are statistically significant (~12% Crete). Only in southwestern Greece and in the island stations in the northern Aegean Sea, the model underestimates the raindays – statistically significant results for the stations of Kalamata (–18.1%), Kythira (–15.1%) and Tripoli (–13%) (Figure 12 (a2)).

In spring, both  $P_{500}$  and  $P_{500sc\_SH\_rd}$  methods overestimate the raindays but the positive differences are higher in the latter case ( $P_{500sc\_SH\_rd}$ ), presenting statistically significant results in many stations. In the island station of Milos, the percentage of this overestimation is 32.4% (Table V). On the other hand, regarding  $P_{500}$  only two stations presented differences that are statistically significant, those of Agrinio and Mytilini (Figure 12 (b1,b2)).

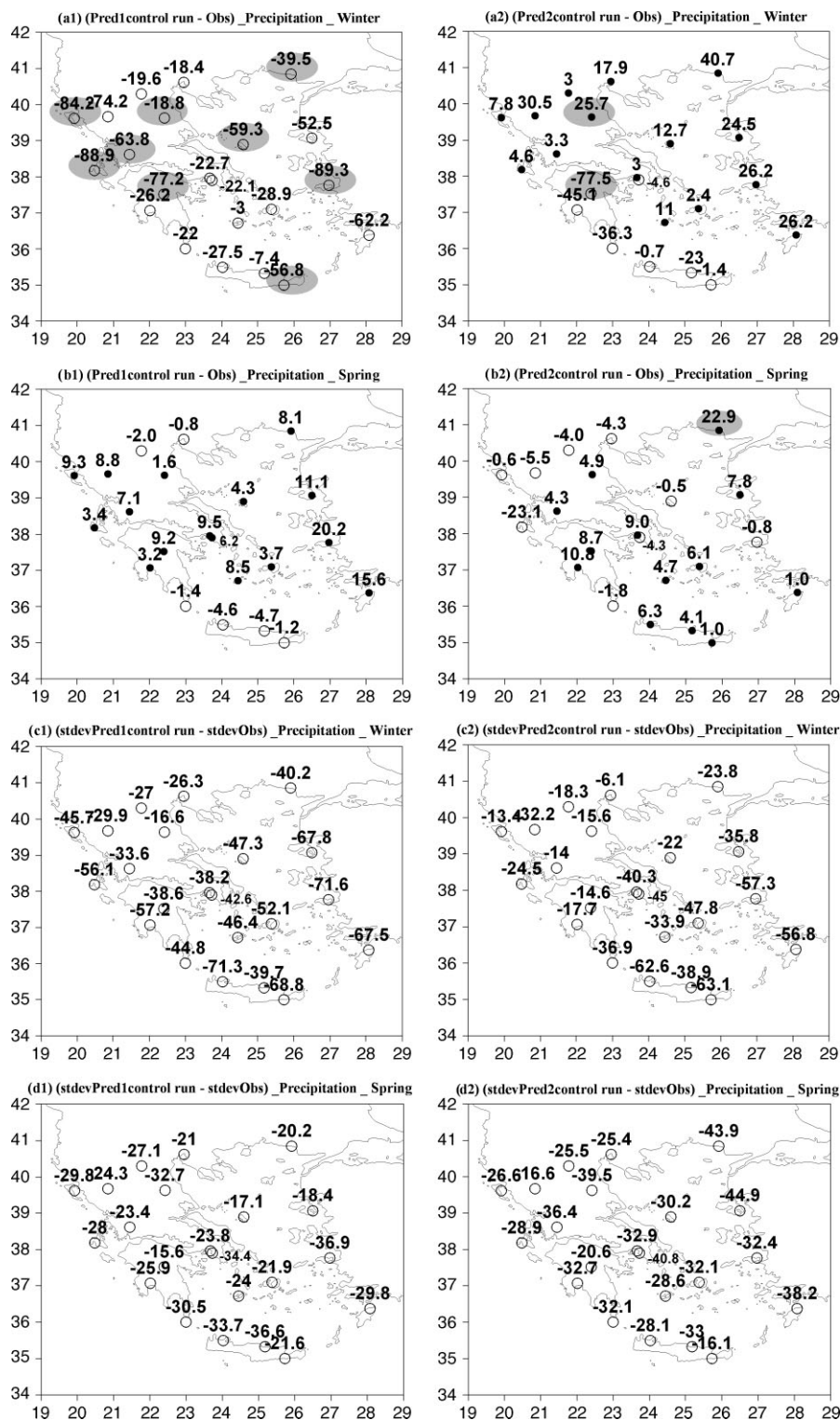


Figure 11. Precipitation and standard deviation differences between the simulated and the station values (simulated – obs) with the GCM predictors (Pred1 =  $P_{500}$ , Pred2 =  $P_{500sc\_SH\_prec}$ ) for the period 1960–1990 for winter and spring. The negative differences are represented by white circles and the positive ones by black circles. The shadowed areas are the statistically significant ones (Student's  $t$ -test).

In an attempt to evaluate the ability of the GCM to reproduce the variability of the seasonal raindays, it was found that the HadAM3P underestimates the standard deviation values both in winter and spring. It is worth noting that in the case of  $P_{500sc\_SH\_rd}$  the negative differences are greater in absolute values, suggesting that the underestimation of the variability is higher

as compared to the  $P_{500}$  case (Figure 12 (c1, c2 – d1, d2)).

#### *HadAM3P results for the future scenario 2070–2100. Precipitation – raindays*

In this section, the changes in seasonal precipitation and raindays are estimated for the future period

Table IV. Observed and simulated seasonal rainfall amounts using the HadAM3P control run for the period 1960–1990 for the two sets of predictors. The columns in italics present the percentage of the differences (%).

	Winter					Spring				
	Obs	P <sub>500</sub>		P <sub>500sc_SH-prec</sub>		Obs	P <sub>500</sub>		P <sub>500sc_SH-prec</sub>	
		C. run	% Diff	C. Run	% Diff		C. run	% Diff	C. run	% Diff
Agrinio	387.2	323.4	<i>-16.5</i>	390.5	<i>0.9</i>	175.2	182.3	<i>4.1</i>	179.5	<i>2.5</i>
Alexand.	208.8	169.3	<i>-18.9</i>	249.5	<i>19.5</i>	127.2	135.3	<i>6.4</i>	150.1	<i>18.0</i>
Argostoli	423	334.1	<i>-21.0</i>	427.6	<i>1.1</i>	161.1	164.5	<i>2.1</i>	138.0	<i>-14.3</i>
Athens	160.7	138	<i>-14.1</i>	163.7	<i>1.9</i>	85.2	94.7	<i>11.2</i>	94.2	<i>10.6</i>
Chania	322.7	295.2	<i>-8.5</i>	322.0	<i>-0.2</i>	122.9	118.3	<i>-3.7</i>	129.2	<i>5.1</i>
Elliniko	160.7	138.6	<i>-13.8</i>	156.1	<i>-2.9</i>	87.4	93.6	<i>7.1</i>	83.1	<i>-4.9</i>
Heraklio	247	239.6	<i>-3.0</i>	224.0	<i>-9.3</i>	104.6	99.9	<i>-4.5</i>	108.7	<i>3.9</i>
Ierapetra	295.5	238.7	<i>-19.2</i>	294.1	<i>-0.5</i>	84.8	83.6	<i>-1.4</i>	85.8	<i>1.2</i>
Ioannina	417.3	343.1	<i>-17.8</i>	447.8	<i>7.3</i>	247.4	256.2	<i>3.6</i>	241.9	<i>-2.2</i>
Kalamata	361.8	335.6	<i>-7.2</i>	316.7	<i>-12.5</i>	143	146.2	<i>2.2</i>	153.8	<i>7.6</i>
Kerkyra	449.5	365.3	<i>-18.7</i>	457.3	<i>1.7</i>	198.2	207.5	<i>4.7</i>	197.6	<i>-0.3</i>
Kozani	121.8	102.2	<i>-16.1</i>	124.8	<i>2.5</i>	142.6	140.6	<i>-1.4</i>	138.6	<i>-2.8</i>
Kythira	287.3	265.3	<i>-7.7</i>	251.0	<i>-12.6</i>	97.2	95.8	<i>-1.4</i>	95.4	<i>-1.9</i>
Larissa	124.2	105.4	<i>-15.1</i>	149.9	<i>20.7</i>	110.4	112.0	<i>1.4</i>	115.3	<i>4.4</i>
Milos	216.1	213.1	<i>-1.4</i>	227.1	<i>5.1</i>	82.5	91.0	<i>10.3</i>	87.2	<i>5.7</i>
Mytilini	366.6	314.1	<i>-14.3</i>	391.1	<i>6.7</i>	143.9	155.0	<i>7.7</i>	151.7	<i>5.4</i>
Naxos	198.4	169.5	<i>-14.6</i>	200.8	<i>1.2</i>	77.5	81.2	<i>4.8</i>	83.6	<i>7.9</i>
Rodos	421.7	359.5	<i>-14.7</i>	447.9	<i>6.2</i>	117.8	133.4	<i>13.2</i>	118.8	<i>0.8</i>
Samos	461.8	372.5	<i>-19.3</i>	488.0	<i>5.7</i>	152.7	172.9	<i>13.2</i>	151.9	<i>-0.5</i>
Skyros	218.7	159.4	<i>-27.1</i>	231.4	<i>5.8</i>	89.8	94.1	<i>4.8</i>	89.3	<i>-0.6</i>
Thess.	125.5	107.1	<i>-14.7</i>	143.4	<i>14.3</i>	131.2	130.4	<i>-0.6</i>	126.9	<i>-3.3</i>
Tripoli	365.6	288.4	<i>-21.1</i>	288.1	<i>-21.2</i>	168.8	178.0	<i>5.5</i>	177.5	<i>5.2</i>

Table V. As in Table IV but for seasonal raindays.

	Winter					Spring				
	Obs	P <sub>500</sub>		P <sub>500sc_SH-rd</sub>		Obs	P <sub>500</sub>		P <sub>500sc_SH-rd</sub>	
		C. run	% Diff	C. run	% Diff		C. run	% Diff	C. run	% Diff
Agrinio	37.1	33.3	<i>-10.2</i>	36.9	<i>-0.5</i>	26.3	28.9	<i>9.9</i>	32.1	<i>22.1</i>
Alexand.	28.1	23.5	<i>-16.4</i>	28.3	<i>0.7</i>	23.2	25.3	<i>9.1</i>	27.1	<i>16.8</i>
Argostoli	43.5	36	<i>-17.2</i>	45.1	<i>3.7</i>	23.9	26.7	<i>11.7</i>	27.3	<i>14.2</i>
Athens	28.2	25	<i>-11.3</i>	30.4	<i>7.8</i>	19.5	20.9	<i>7.2</i>	24.1	<i>23.6</i>
Chania	41.6	38.4	<i>-7.7</i>	47.2	<i>13.5</i>	19.5	20.8	<i>6.7</i>	24.5	<i>25.6</i>
Elliniko	27	24.2	<i>-10.4</i>	29.8	<i>10.4</i>	18.5	19.5	<i>5.4</i>	23.4	<i>26.5</i>
Heraklio	36.8	35.8	<i>-2.7</i>	41.1	<i>11.7</i>	17.7	19.3	<i>9.0</i>	20.1	<i>13.6</i>
Ierapetra	34.9	31.7	<i>-9.2</i>	39.2	<i>12.3</i>	13.4	14	<i>4.5</i>	16	<i>19.4</i>
Ioannina	38.4	33.8	<i>-12.0</i>	39.6	<i>3.1</i>	34	36.2	<i>6.5</i>	40	<i>17.6</i>
Kalamata	41.9	37.7	<i>-10.0</i>	34.3	<i>-18.1</i>	24.8	26.5	<i>6.9</i>	29	<i>16.9</i>
Kerkyra	42.3	36.2	<i>-14.4</i>	42	<i>-0.7</i>	28.4	30.4	<i>7.0</i>	30.9	<i>8.8</i>
Kozani	26.3	22.8	<i>-13.3</i>	26.3	<i>0.0</i>	28	28.8	<i>2.9</i>	28.2	<i>0.7</i>
Kythira	38.5	33.2	<i>-13.8</i>	32.7	<i>-15.1</i>	17.3	18.4	<i>6.4</i>	20.1	<i>16.2</i>
Larissa	27	24.9	<i>-7.8</i>	30.6	<i>13.3</i>	24.8	27.7	<i>11.7</i>	26.3	<i>6.0</i>
Milos	31.4	29.7	<i>-5.4</i>	35.3	<i>12.4</i>	14.2	16	<i>12.7</i>	18.8	<i>32.4</i>
Mytilini	33.3	29.7	<i>-10.8</i>	33	<i>-0.9</i>	20.8	23.6	<i>13.5</i>	19.7	<i>-5.3</i>
Naxos	33.6	30.2	<i>-10.1</i>	36.3	<i>8.0</i>	16	17.6	<i>10.0</i>	15	<i>-6.3</i>
Rodos	39.7	34.7	<i>-12.6</i>	43.1	<i>8.6</i>	17.9	19.4	<i>8.4</i>	18.6	<i>3.9</i>
Samos	36.8	33.5	<i>-9.0</i>	40.8	<i>10.9</i>	19.5	21.9	<i>12.3</i>	22.1	<i>13.3</i>
Skyros	31.1	26.5	<i>-14.8</i>	29.2	<i>-6.1</i>	16.6	18.6	<i>12.0</i>	18.4	<i>10.8</i>
Thess.	28.7	23.6	<i>-17.8</i>	31	<i>8.0</i>	28	29.4	<i>5.0</i>	28.4	<i>1.4</i>
Tripoli	39.9	33	<i>-17.3</i>	34.7	<i>-13.0</i>	29.7	31.5	<i>6.1</i>	30.8	<i>3.7</i>

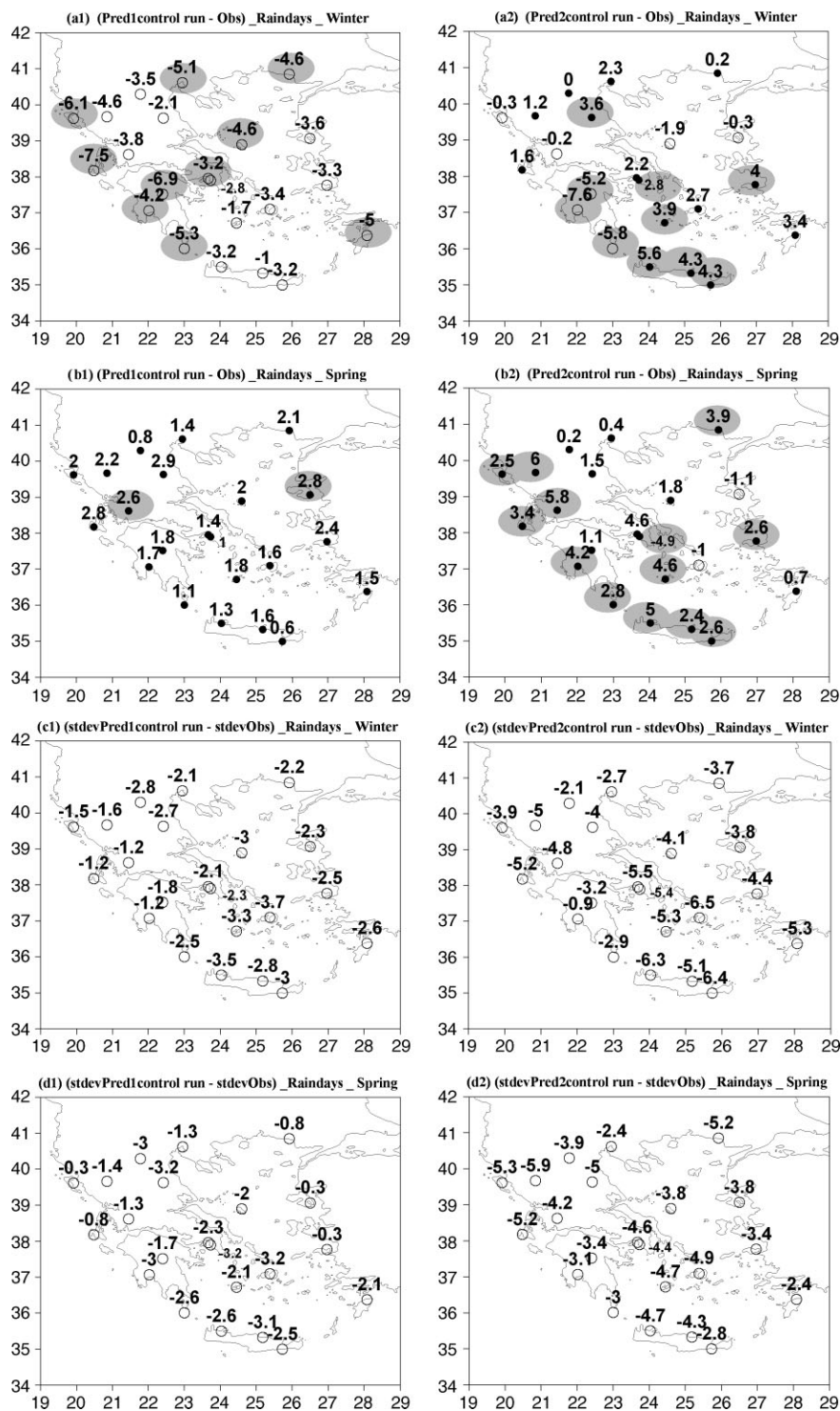


Figure 12. As in Figure 11 but for the seasonal raindays.

2070–2100. These changes have been derived from the indirect results obtained through the application of the downscaling model. The differences between the scenario and the control run were calculated using both approaches ( $P_{500}$  and  $P_{500sc\_SH\_prec}/rd$ ) and are compared to the seasonal changes obtained directly from the HadAM3P output.

Winter precipitation (Table VI, Figure 13) presents a substantial decrease in the largest part of the Greek area using both sets of predictors. More specifically, the  $P_{500}$

results show that the greatest decrease will appear in the southern parts of the country, while on the other hand, northwestern continental Greece will experience a small increase in the rainfall amounts. Using  $P_{500sc\_SH\_prec}$ , the greatest negative differences are observed in western Greece and in the eastern Aegean Sea and only Crete presents a small increase. The higher amplitude of the changes in  $P_{500sc\_SH\_prec}$  could be interpreted partially from the behavior of the predictors. The downscaling model reproduced smaller future precipitation values

when specific humidity and raw precipitation data were used as predictors, in comparison to the simulated precipitation values found when 500 hPa geopotential heights were used as the only predictor. Table VI depicts the percentage of change predicted by the two downscaling approaches.

The comparison of the above results with the respective differences derived from the direct output of the GCM (Figure 13 (a3)) shows that the downscaled model simulates changes, which are in general in the same direction as the HadAM3P ones (decrease of precipitation) but the magnitude of the differences is not in accordance with the simulated indirect results. The increase in the precipitation amounts in northwestern Greece for the P<sub>500</sub> method, which are in contrast to the GCM results, suggests that the changes in winter precipitation cannot be described completely from the changes in the geopotential heights at the 500 hPa level.

The downscaled results obtained in the case of spring show that the model predicts a decrease of precipitation with both approaches for the whole study area (Figure 13 (b1–b2)). The largest negative differences were found in northwestern Greece and in the eastern Aegean islands when P<sub>500</sub> is used: for Samos  $\sim -26\%$  decrease of precipitation is predicted (Table VI). The aforementioned areas as well as Crete will experience the greatest precipitation decrease according to P<sub>500sc\_SH\_prec</sub>. Similar to winter, the GCM predicts a decrease in spring precipitation but

this time the amplitude of the differences is higher than that of the downscaled results (Figure 13 (b3)). Although the geopotential heights from the scenario present higher values ( $\sim 80$  gpm) than the corresponding ones from the control run this increase could not account for the reproduction of such low precipitation totals.

Figure 14 depicts the indirect and direct differences (scenario-control run) for the future period 2070–2100 for seasonal raindays while Table VII shows the percentage of the predicted changes. In the case of winter, discrepancies can be detected between the downscaled and the GCM results. The downscaling model with P<sub>500</sub> predicts a decrease in the number of raindays in the Aegean Sea and mainly in Crete – in Ierapetra raindays will decrease about  $-16\%$ . On the contrary, in central and western continental Greece a small increase in the number of raindays is expected (Figure 14 (a1)). This change in raindays is almost identical to the predicted future changes of winter precipitation. Using P<sub>500sc\_SH\_rd</sub>, the calculated differences show an increase of raindays in western Greece and the central northeastern Aegean Sea. In the rest of the country, raindays will decrease. The greatest negative differences were found in the southwest and in Macedonia (Figure 14 (a2)). The GCM (Figure 14 (a3)) predicts a general decrease of the raindays in the study area, especially for the grid point in Macedonia and Thessaly. The magnitude of the differences is higher than the downscaled results, mainly the

Table VI. Seasonal future (scenario) and present day (control run) precipitation amounts using the HadAM3P data for the two sets of predictors. The columns in italics depict the percentage of the predicted change.

	Winter						Spring					
	P <sub>500</sub>			P <sub>500sc_SH_prec</sub>			P <sub>500</sub>			P <sub>500sc_SH_prec</sub>		
	Scen.	C. run	% change	Scen.	C. run	% change	Scen.	C. run	% change	Scen.	C. run	% change
Agrinio	332.4	323.4	2.8	342.5	390.5	<i>-12.3</i>	171.3	182.3	<i>-6.0</i>	166.7	179.5	<i>-7.1</i>
Alexand.	169.8	169.3	<i>0.3</i>	170.4	249.5	<i>-31.7</i>	107.8	135.3	<i>-20.3</i>	141.7	150.1	<i>-5.6</i>
Argostoli	326.0	334.1	<i>-2.4</i>	373.3	427.6	<i>-12.7</i>	152.0	164.5	<i>-7.6</i>	131.7	138.0	<i>-4.6</i>
Athens	119.9	138.0	<i>-13.1</i>	158.7	163.7	<i>-3.1</i>	84.2	94.7	<i>-11.1</i>	91.4	94.2	<i>-3.0</i>
Chania	215.0	295.2	<i>-27.2</i>	322.7	322.0	<i>0.2</i>	116.1	118.3	<i>-1.9</i>	115.2	129.2	<i>-10.8</i>
Elliniko	126.1	138.6	<i>-9.0</i>	151.5	156.1	<i>-2.9</i>	83.2	93.6	<i>-11.1</i>	82.2	83.1	<i>-1.1</i>
Heraklio	189.4	239.6	<i>-21.0</i>	224.8	224.0	<i>0.4</i>	97.3	99.9	<i>-2.6</i>	93.1	108.7	<i>-14.4</i>
Ierapetra	197.3	238.7	<i>-17.3</i>	295.0	294.1	<i>0.3</i>	75.2	83.6	<i>-10.0</i>	78.6	85.8	<i>-8.4</i>
Ioannina	340.0	343.1	<i>-0.9</i>	398.5	447.8	<i>-11.0</i>	221.6	256.2	<i>-13.5</i>	230.1	241.9	<i>-4.9</i>
Kalamata	341.9	335.6	<i>1.9</i>	255.5	316.7	<i>-19.3</i>	140.9	146.2	<i>-3.6</i>	154.1	153.8	<i>0.2</i>
Kerkyra	369.6	365.3	<i>1.2</i>	398.6	457.3	<i>-12.8</i>	182.6	207.5	<i>-12.0</i>	186.7	197.6	<i>-5.5</i>
Kozani	103.9	102.2	<i>1.7</i>	90.4	124.8	<i>-27.6</i>	138.0	140.6	<i>-1.8</i>	124.4	138.6	<i>-10.2</i>
Kythira	233.5	265.3	<i>-12.0</i>	230.3	251.0	<i>-8.2</i>	87.8	95.8	<i>-8.4</i>	102.5	95.4	<i>7.4</i>
Larissa	104.3	105.4	<i>-1.0</i>	128.3	149.9	<i>-14.4</i>	112.4	112.0	<i>0.4</i>	104.8	115.3	<i>-9.1</i>
Milos	183.3	213.1	<i>-14.0</i>	223.3	227.1	<i>-1.7</i>	79.3	91.0	<i>-12.9</i>	85.7	87.2	<i>-1.7</i>
Mytilini	292.9	314.1	<i>-6.7</i>	266.3	391.1	<i>-31.9</i>	126.4	155.0	<i>-18.5</i>	139.4	151.7	<i>-8.1</i>
Naxos	149.8	169.5	<i>-11.6</i>	196.2	200.8	<i>-2.3</i>	62.9	81.2	<i>-22.5</i>	76.3	83.6	<i>-8.7</i>
Rodos	355.7	359.5	<i>-1.1</i>	412.5	447.9	<i>-7.9</i>	101.2	133.4	<i>-24.1</i>	102.7	118.8	<i>-13.6</i>
Samos	357.9	372.5	<i>-3.9</i>	448.9	488.0	<i>-8.0</i>	128.5	172.9	<i>-25.7</i>	128.0	151.9	<i>-15.7</i>
Skyros	129.2	159.4	<i>-18.9</i>	146.5	231.4	<i>-36.7</i>	72.2	94.1	<i>-23.3</i>	82.0	89.3	<i>-8.2</i>
Thess.	109.2	107.1	<i>2.0</i>	109.3	143.4	<i>-23.8</i>	119.3	130.4	<i>-8.5</i>	113.5	126.9	<i>-10.6</i>
Tripoli	256.1	288.4	<i>-11.2</i>	241.8	288.1	<i>-16.1</i>	162.6	178.0	<i>-8.7</i>	171.9	177.5	<i>-3.2</i>

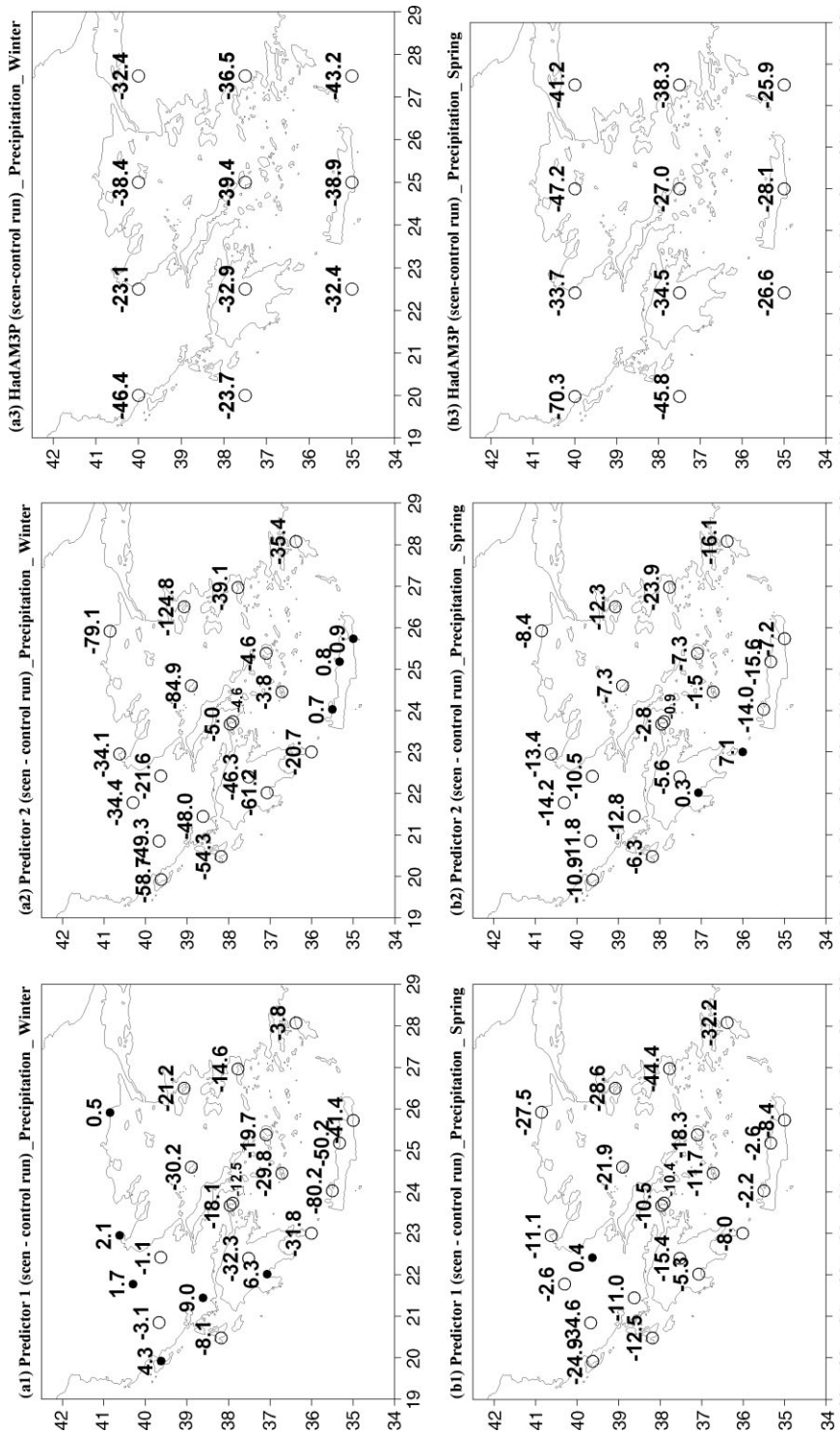


Figure 13. Estimations of the future precipitation changes from the downscaled results (columns 1, 2) and the direct output from the GCM (column 3). The differences have been calculated (scenario – control run) and the negative differences are represented in white circles and the positive ones with black circles.

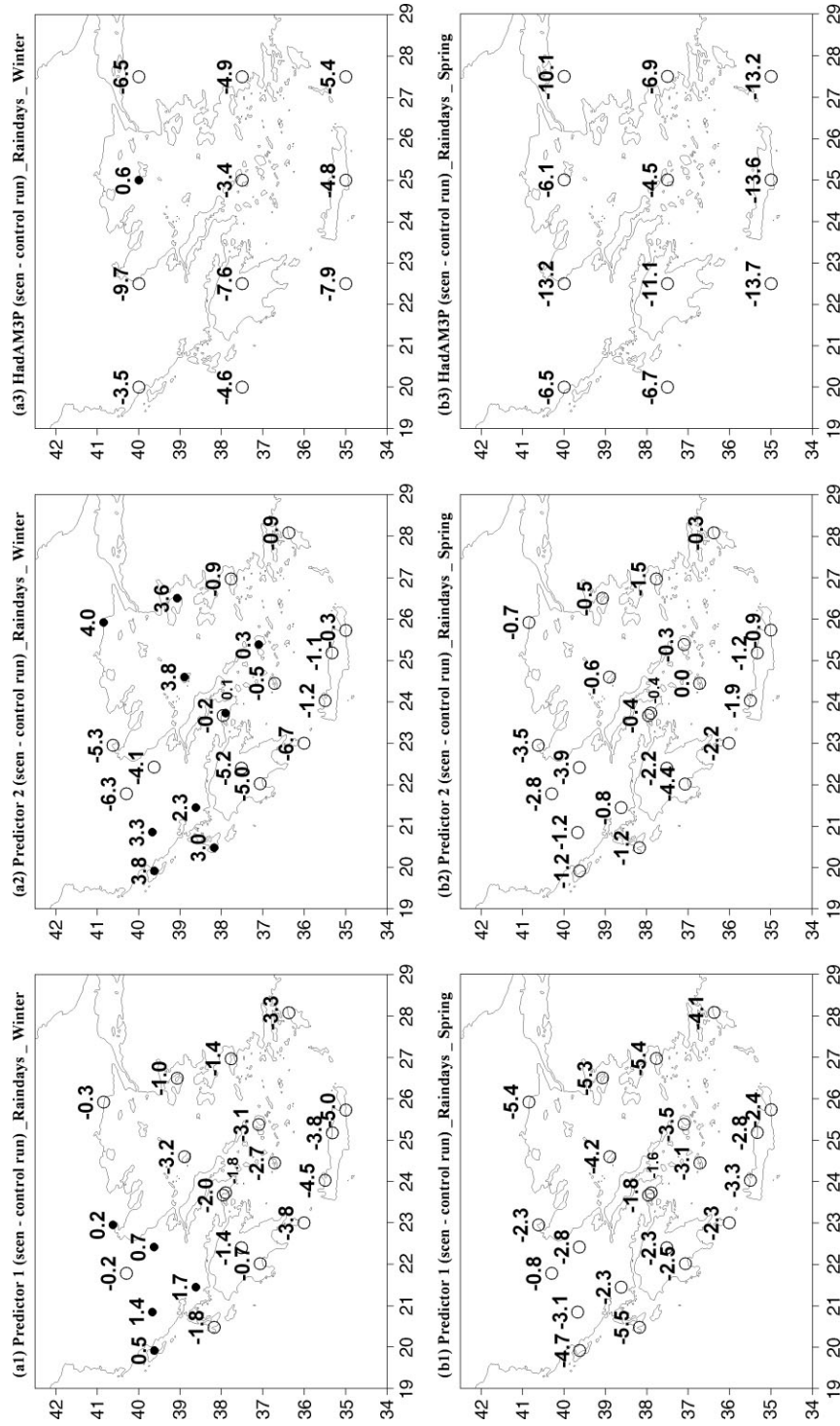


Figure 14. As in Figure 13 but for estimations for the future raindays change.

Table VII. As in Table VI but for the seasonal raindays.

	Winter						Spring					
	P <sub>500</sub>			P <sub>500sc_SH_rld</sub>			P <sub>500</sub>			P <sub>500sc_SH_rld</sub>		
	Scen.	C. run	% change	Scen.	C. run	% change	Scen.	C. run	% change	Scen.	C. run	% change
Agrinio	35	33.3	5.1	39.2	36.9	6.2	26.6	28.9	-8.0	31.3	32.1	-2.5
Alexand.	23.2	23.5	-1.3	32.3	28.3	14.1	19.9	25.3	-21.3	26.4	27.1	-2.6
Argostoli	34.2	36	-5.0	48.1	45.1	6.7	21.2	26.7	-20.6	26.1	27.3	-4.4
Athens	23	25	-8.0	30.2	30.4	-0.7	19.1	20.9	-8.6	23.7	24.1	-1.7
Chania	33.9	38.4	-11.7	46	47.2	-2.5	17.5	20.8	-15.9	22.6	24.5	-7.8
Elliniko	22.4	24.2	-7.4	29.9	29.8	0.3	17.9	19.5	-8.2	23	23.4	-1.7
Heraklio	32	35.8	-10.6	40	41.1	-2.7	16.5	19.3	-14.5	18.9	20.1	-6.0
Ierapetra	26.7	31.7	-15.8	38.9	39.2	-0.8	11.6	14	-17.1	15.1	16	-5.6
Ioannina	35.2	33.8	4.1	42.9	39.6	8.3	33.1	36.2	-8.6	38.8	40	-3.0
Kalamata	37	37.7	-1.9	29.3	34.3	-14.6	24	26.5	-9.4	24.6	29	-15.2
Kerkyra	36.7	36.2	1.4	45.8	42	9.0	25.7	30.4	-15.5	29.7	30.9	-3.9
Kozani	22.6	22.8	-0.9	20	26.3	-24.0	28	28.8	-2.8	25.4	28.2	-9.9
Kythira	29.4	33.2	-11.4	26	32.7	-20.5	16.1	18.4	-12.5	17.9	20.1	-10.9
Larissa	25.6	24.9	2.8	26.5	30.6	-13.4	24.9	27.7	-10.1	22.4	26.3	-14.8
Milos	27	29.7	-9.1	34.8	35.3	-1.4	12.9	16	-19.4	18.8	18.8	0.0
Mytilini	28.7	29.7	-3.4	36.6	33	10.9	18.3	23.6	-22.5	19.2	19.7	-2.5
Naxos	27.1	30.2	-10.3	36.6	36.3	0.8	14.1	17.6	-19.9	14.7	15	-2.0
Rodos	31.4	34.7	-9.5	42.2	43.1	-2.1	15.3	19.4	-21.1	18.3	18.6	-1.6
Samos	32.1	33.5	-4.2	39.9	40.8	-2.2	16.5	21.9	-24.7	20.6	22.1	-6.8
Skyros	23.3	26.5	-12.1	33	29.2	13.0	14.4	18.6	-22.6	17.8	18.4	-3.3
Thess.	23.8	23.6	0.8	25.7	31	-17.1	27.1	29.4	-7.8	24.9	28.4	-12.3
Tripoli	31.6	33	-4.2	29.5	34.7	-15.0	29.2	31.5	-7.3	28.6	30.8	-7.1

ones derived using P<sub>500</sub>, probably resulting from the small sensitivity of the 500 hPa geopotential heights to greenhouse forcing.

While for spring HadAM3P predicts a strong decrease of raindays of 5–13 days throughout the future period, the statistical model predicts smaller changes as with the same sign with the GCM (decrease of raindays, Figure 14 (b1–b3)). The P<sub>500</sub> application gave differences that reach the value of -5 raindays in western and eastern Greece. The differences found using P<sub>500sc\_SH\_rld</sub> are even smaller (-4 raindays in Peloponnissos and Thessaly).

## CONCLUSIONS AND DISCUSSION

In the present study, a statistical downscaling model based on the ANN approach was constructed to find empirical relationships between large-scale variables (predictors) and observational precipitation and raindays (predictants) over the Greek area, for winter, spring and autumn (not presented). As a first step a circulation-based predictor was chosen -500 hPa geopotential heights (NCEP reanalysis data) - and the results of the downscaling model were evaluated against station data. The model was trained for a period of 27 years (1958–1978 to 1994–2000) and validated for the intermediate period, 1979–1993. The performance of the downscaling model was assessed by means of correlation coefficient values, RMSE values and mean and standard deviation differences.

It was found that the ANN approach was able to reproduce satisfactorily the observed parameters for winter and spring (high correlations). In the case of autumn the model's effectiveness was found to be poor and the results were moderate and less accurate, especially in comparison to winter results, so they were not presented in the current study. This could be attributed to the fact that the atmospheric circulation during the winter season is more intense, less variable and plays a more predominant role in precipitation than other smaller factors, such as convection or topography. Furthermore, the 500 hPa field produced by the model appears to have such large variability as compared to the other seasons that the simulation of autumn precipitation is far more difficult (Maheras *et al.*, 2004).

The difficulty in reproducing autumn precipitation was also noted in the Maheras *et al.* (2004) study where a statistical downscaling technique based on a circulation type approach was applied. The downscaling technique was found to be weak in capturing well the natural variability of the observed time series (underestimation of the standard deviation values), suggesting that it is unable to generate the extreme precipitation events (Wilby *et al.*, 1998; Maheras *et al.*, 2004). However, its performance in reproducing the evolution time of the series was very high (for winter and spring).

The reproduction of the actual magnitudes of the precipitation total and the number of raindays varied from station to station and from season to season. Although,

the spatial coherence of our results would be preferred, the sharp and complex orography of the Greek area, including mountainous areas and numerous islands, lead to a relative random distribution of positive and negative differences. Despite this fact, especially in the case of winter the results demonstrate some spatial coherence where areas with positive and negative differences are quite well distinguished.

The differences between the simulated and the observed precipitation totals are in some case quite large; however, previous studies based on ANNs demonstrated similar or even larger differences in other regions (Cavazos, 1997). This could be attributed to both on the complexity of the methodology and the variability of the precipitation regime. Generally, the raindays were better reproduced than the seasonal precipitation, which could be attributed to the fact that the occurrence of rainfall (raindays) is more strongly correlated to the 500 hPa circulation than the actual precipitation values (Maheras and Anagnostopoulou, 2003).

Comparing the Maheras *et al.* (2004) circulation type based approach with the ANN approach, which were validated for the same time period and for the same data, it can be concluded that the neural network approach presented higher correlations and lower RMSE values. On the other hand, the circulation type approach was found to be more suitable in simulating the actual rainfall amounts and the variability of the time series (smaller mean and st dev differences). Therefore, it is suggested that there cannot be a clear recommendation of which statistical downscaling method is the most appropriate, since each one has its own advantages and limitations.

According to Hewitson and Crane (1996) and Crane and Hewitson (1998) the use of additional, alternative predictors could make an impact on the final results when ANN models are applied in a downscaling procedure. Thus, apart from the 500 hPa, two other predictors, surface specific humidity and raw precipitation, were selected for specific grid points. Specific humidity is considered to be a measure of the absolute moisture content of the atmosphere. Also, combining raw precipitation data with circulation data as predictors would include thermodynamic and fluid dynamic controls on precipitation (Salathé, 2003). The addition of this set of predictors to the ANN model revealed improved results in most of the cases, with higher correlation coefficients, lower RMSE values and smaller mean and standard deviation differences. This is in agreement with other studies where precipitation was used as a predictor (Widmann *et al.*, 2003; Salathé, 2003; Schmidli *et al.*, 2005) further confirming that simulated precipitation is an appropriated predictor for the observational precipitation.

Overall, since our downscaling procedure appeared to be suitable in generating estimations of precipitation and raindays series, mainly for winter and spring, the same transfer functions were applied to present day (control

run) and future scenarios from the atmospheric model HadAM3P.

The results of the downscaling model using the GCM predictor sets ( $P_{500}$  and  $P_{500sc\_SH\_prec/rd}$ ) for the present period (1960–1990) were found to be quite different. For example, while using GCM  $P_{500}$  an underestimation of winter precipitation was detected, and the GCM  $P_{500sc\_SH\_prec}$  simulated overestimated rainfall totals in the largest part of the country. Similar results were deduced for the simulated raindays. This is not surprising since the capability of the GCM to simulate realistically the predictors should be taken into consideration. Different sets of predictors could give different simulated results as different GCMs may produce different results even if the same downscaling procedure is used (von Storch *et al.*, 1993).

Finally, the changes in seasonal precipitation and raindays were estimated for the future HadAM3P scenario based on the A2 IPCC experiment. The downscaled results were compared with the direct results from the GCM. Comparisons of this kind are meaningful when the downscaling model is proved to be skilful and for a reliable GCM (Busuioc *et al.*, 1999). Generally, a good agreement was observed between the scenarios obtained from the GCM direct output and by downscaling. The climate change signal for both precipitation and raindays, especially for spring, is similar for the GCM and the downscaling model, predicting a decrease of the parameters in the Greek area. However, the magnitude of changes tends to be different. Although the downscaling model was successful in using station data, this does not constitute an affirmation that the results obtained for different future climate conditions would be always valid. Even though one of the most important assumptions of any statistical downscaling technique is the stationarity of the parameters used (Wilby, 1997), there is no assurance that the relationship of the predictors and the predictants will not change in the future (Maheras *et al.*, 2004). In this sense, the downscaled results should be interpreted cautiously (Charles *et al.*, 1999).

As a future work, the authors plan to incorporate further large-scale predictors, which could contribute to a more satisfying reproduction of the variability of precipitation, as well as the improvement of the model ability to better reproduce the actual rainfall values. Also, our study will of the success improve the assessment the downscaling model in simulating finer timescale data as monthly or daily.

#### ACKNOWLEDGEMENTS

This work was funded by the Commission of the European Union under the STARDEX (Statistical and Regional Dynamical Downscaling of Extremes for European Regions) contract (EVK2-CT-2001-00115). The authors would like to express their gratitude to the reviewers for their constructive comments and suggestions.

## REFERENCES

- Alexandersson H. 1986. A homogeneity test applied to precipitation data. *Journal of Climatology* **6**: 661–675.
- Busuioc A, von Storch H, Schnur R. 1999. Verification of GCM-generated regional seasonal precipitation for current climate and of statistical downscaling estimates under changing climate conditions. *Journal of Climate* **12**: 258–272.
- Busuioc A, Deliang C, Hellstrom C. 2001. Performance of statistical Downscaling models in GCM validation and regional climate change estimates: application for Swedish precipitation. *International Journal of Climatology* **21**: 557–578.
- Cavazos T. 1997. Downscaling large-scale circulation to local winter Rainfall in north-eastern Mexico. *International Journal of Climatology* **17**: 1069–1082.
- Charles SP, Bryson CB, Whetton PH, Hughes JP. 1999. Validation of downscaling models for changed climate conditions: case study of southwestern Australia. *Climate Research* **12**: 1–14.
- Corte-Real D, Zhang X, Wang C. 1995. Large-scale circulation regimes and surface climatic anomalies over the Mediterranean. *International Journal of Climatology* **15**: 1135–1150.
- Crane RG, Hewitson BC. 1998. Doubled CO<sub>2</sub> Precipitation changes for the Susquehanna Basin: downscaling from the Genesis General Circulation Model. *International Journal of Climatology* **18**: 64–76.
- Cubash U, Meehl GA, Boer GJ, Stouffer MD, Noda A, Senior CA, Raper S, Yap KS. 2001. Projections of Future Climate Change. In IPCC WG1 TAR, 2001.
- Fahlman S. 1988. Faster learning variations on Back-propagation. *An Empirical Study. Proceedings of 1988 Connectionist Models Summer School*. published by Morgan Kaufmann: Carnegie Mellon University, Pittsburgh, PA.
- Freeman JA, Skapura DM. 1991. *Neural Networks. Algorithms, Applications and Programming Techniques*. Addison-Wesley Publishing Company: Menlo Park, California, USA; 393.
- González-Rouco JF, Heyen H, Zorita E, Valero F. 2000. Agreement between Observed Rainfall Trends and Climate Change Simulations in the Southwest of Europe. *Journal of Climate* **13**: 3057–3065.
- Goodess CM, Palutikof JP. 1998. Development of Daily Rainfall Scenarios for southeast Spain using a circulation – type approach downscaling. *International Journal of Climatology* **10**: 1051–1083.
- Goodess CM, Anagnostopoulou C, Bårdossy A, Frei C, Harpham C, Haylock MR, Hundecha Y, Maheras P, Ribalaygue J, Schmidli J, Schmith T, Tolika K, Tomozeiu R, Wilby RL. 2006. An intercomparison of statistical downscaling methods for Europe and European regions-assessing their performance with respect to extreme temperature and precipitation events. *Climatic Change Accepted*.
- Gyalistras D, von Storch H, Fischlin A, Beniston M. 1994. Linking GCM-simulated climatic changes to ecosystem models: case studies of statistical downscaling in the Alps. *Climate Research* **4**: 167–189.
- Haylock MR, Cawley GC, Harpham C, Wilby RL, Goodess CM. 2006. Downscaling heavy precipitation over the United Kingdom: A comparison of dynamical and statistical methods and their future scenarios. *International Journal of Climatology* **25**(10): 1397–1415.
- Hewitson BC, Crane RG. 1996. Climate downscaling: techniques and application. *Climate Research* **7**: 85–95.
- Jones R, Murphy J, Hassell D, Taylor R. 2001. *Ensemble Mean Changes in a Simulation of the European Climate of 2071–2100 Using the New Hadley Centre Regional Modelling System HadAM3H/HadRM3H*. Hadley Centre, Met Office: Bracknell.
- Kalnay E, Kanamitsou M, Kistler R, Collins W, Deaven D, Gandin L, Irebell M, Saha S, White G, Woollen J, Zhu Y, Leetmaa A, Reynolds R, Chelliah M, Ebisuzaki W, Huggins W, Janowiak J, Mo KC, Ropelewski C, Wang J, Jenne R, Joseph D. 1996. The NCEP/NCAR 40-year Reanalysis project. *Bulletin of the American Meteorological Society* **77**: 437–471.
- Kidson JW, Thompson CS. 1998. A comparison of statistical and model – based downscaling techniques for estimating local climate variations. *Journal of Climate* **11**: 735–753.
- Kilsby CG, Cowpertwait PSP, O’Connell PE, Jones PD. 1998. Predicting rainfall statistics in England and Wales using atmospheric circulation variables. *International Journal of Climatology* **18**: 523–539.
- Knutti R, Stocker TR, Joos F, Plattner GK. 2003. Probabilistic climate change projections using neural networks. *Climate Dynamics* **21**: 257–272.
- Kostopoulou E, Giannakopoulos C, Anagnostopoulou C, Tolika K, Maheras P, Vafiadis M. 2005. Simulating maximum and minimum temperatures over Greece: a comparison of three modeling techniques, Submitted for publication on the Climate Research.
- Koutsoukios I, Rapsomanikis S, Loupa R. 2006. Robust stochastic seasonal precipitation scenarios. *International Journal of Climatology* **26**(14): 2077–2095.
- Kysely J. 2002. Comparison of extremes in GCM-simulated downscaled and observed central – European temperature series. *Climate Research* **20**: 211–222.
- Maheras P, Anagnostopoulou C. 2003. *Circulation Types and their Influence on the Interannual Variability and Precipitation Changes in Greece. Mediterranean Climate-Variability and Trends*, Bolle HJ (ed.). Springer Verlag: Berlin, Heidelberg; 215–239.
- Maheras P, Tolika K, Anagnostopoulou Chr, Vafiadis M, Patrikas I, Flocas H. 2004. On the Relationships between circulation types and changes in rainfall variability in Greece. *International Journal of Climatology* **24**: 1695–1712.
- Marzban C. 2003. Neural networks for postprocessing model output: ARPS. *Monthly Weather Review* **131**: 1103–1111.
- Pope VD, Gallani ML, Rowntree PR, Stratton RA. 2000. The impact of new physical parametrizations in the Hadley Center climate model: HadAM3. *Climate Dynamics* **16**: 123–146.
- Salathé JREP. 2003. Comparison of various precipitation downscaling methods for the simulation of Streamflow in a Rainshadow River Basin. *International Journal of Climatology* **23**: 887–901.
- Schmidli J, Frei C, Widale PL. 2005. Downscaling from GCM precipitation: a benchmark for dynamical and statistical downscaling methods, Submitted for publication on the International Journal of Climatology.
- Solman SA, Nunez MN. 1999. Local estimates of global climate change: a statistical downscaling approach. *International Journal of Climatology* **19**: 835–861.
- Tatli H, Nuzhet Dalfes H, Sibel Mentés S. 2004. A statistical Downscaling Method for monthly total precipitation over Turkey. *International Journal of Climatology* **24**: 161–180.
- Timbal B, Dufour A, McAvaney B. 2003. An estimate of future climate change for western France using a statistical downscaling technique. *Climate Dynamics* **20**: 807–823.
- Tolika K. 2006. Estimation of future climate changes in the Greek area during the 21st century, using general circulation climate models. PhD thesis, Aristotle University of Thessaloniki, Thessaloniki, Greece, 2006, 305, (in Greek).
- Tolika K, Maheras P. 2005. Spatial and temporal characteristics of wet spells in Greece. *Theoretical and Applied Climatology* **81**: 71–85.
- Tolika K, Maheras P, Flocas HA, Arseni – Papadimitriou A. 2006. An evaluation of a General Circulation Model (GCM) and the NCEP-NCAR reanalysis data for winter precipitation in Greece. *International Journal of Climatology* **26**: 935–955.
- Trigo RM, Palutikof JP. 2001. Precipitation Scenarios over Iberia: a Comparison between Direct GCM output and different downscaling techniques. *Journal of Climate* **14**: 4422–4446.
- von Storch H, Zwiers FW. 2001. *Statistical Analysis in Climate Research*. Cambridge University Press: Cambridge, UK; 484.
- von Storch H, Zorita E, Cubarch U. 1993. Downscaling of global climate change estimates to regional scales: an application to Iberian rainfall in wintertime. *Journal of Climate* **6**: 1161–1171.
- Wasserman PD. 1989. *Neural Computing. Theory and Practice*. Van Nostrand Reinhold: New York; 230.
- Widmann M, Bretherton CS. 2000. Validation of mesoscale precipitation in the NCEP reanalysis using a New Gridcell dataset for the Northwestern United States. *Journal of Climate* **13**: 1936–1950.
- Widmann M, Bretherton CS, Salathé EP. 2003. Statistical precipitation downscaling over the Northwestern United States using numerically simulated precipitation as a predictor. *Journal of Climate* **16**: 799–816.
- Wilby RL. 1997. Non-stationarity in daily precipitation series: implications for GCM downscaling using atmospheric circulation indices. *International Journal of Climatology* **17**: 439–545.
- Wilby RL, Wigley TML. 2000. Precipitation predictors for downscaling: observed and general circulation model relationships. *International Journal of Climatology* **20**: 641–664.
- Wilby RL, Wigley TML, Wilks DS, Hewitson BC, Conway D, Jones PD. 1998. Statistical downscaling of general circulation model output: a comparison of methods. *Water Resources Research* **34**: 2995–3008.
- Xoplaki E, Luterbacher J, Burkard R, Patrikas I, Maheras P. 2000. Connection between the large-scale 500 hPa geopotential height fields and precipitation over Greece during wintertime. *Climate Research* **14**: 129–146.